SIAM J. FINANCIAL MATH.
Vol. 6, pp. 685–712

Reduced Basis Methods for Pricing Options with the Black–Scholes and Heston Models*

O. Burkovska†, B. Haasdonk‡, J. Salomon§, and B. Wohlmuth†

Abstract. In this paper, we present a reduced basis method for pricing European and American options based on the Black–Scholes and Heston models. To tackle each model numerically, we formulate the problem in terms of a time-dependent variational equality or inequality. We apply a suitable reduced basis approach for both types of options. The characteristic ingredients used in the method are a combined POD-Greedy and Angle-Greedy procedure for the construction of the primal and dual reduced spaces. Analytically, we prove the reproduction property of the reduced scheme and derive a posteriori error estimators. Numerical examples are provided, illustrating the approximation quality and convergence of our approach for the different option pricing models. Also, we investigate the reliability and effectivity of the error estimators.

Key words. reduced basis methods, model reduction, a posteriori error estimation, option pricing

AMS subject classifications. 35K85, 65K15, 65M15, 91B25

DOI. 10.1137/140981216

1. Introduction.

We consider the problem of European and American option pricing and refer to [1, 26, 45] and the references therein for an introduction into computational methods for option pricing. While European options can be modeled by a parabolic partial differential equation (PDE), American options result in additional inequality constraints. Different models can be used to price European and American options. The simplest ones, e.g., the Black–Scholes model [3], assume that the volatility is constant. However, in most of the cases, the real market violates this assumption due to its stochastic nature. Thus, alternative models which try to capture this phenomenon are frequently used, e.g., the Heston stochastic volatility model [25].

Another difficulty which arises with solving PDEs for option pricing, in particular for pricing American options, is that for most of the models no closed form solution exists. Thus one has to develop appropriate numerical methods. The common methods to solve pricing equations with the Heston model are finite differences (cf. [11, 31, 29, 30]) and finite elements (cf. [10, 35, 49, 53]). We refer the reader to [24] for a possible numerical treatment of basket

*Received by the editors August 6, 2014; accepted for publication (in revised form) May 27, 2015; published electronically August 6, 2015.

http://www.siam.org/journals/sifin/6/98121.html

†Fakultät Mathematik, Technische Universität München, Germany (burkovsk@ma.tum.de, wohlmuth@ma.tum.de). The work of the first author was supported by the International Research Training Group IGDK1754, funded by the German Research Foundation (DFG).

‡Institut für Angewandte Analysis und Numerische Simulation, Universität Stuttgart, Germany (haasdonk@mathematik.uni-stuttgart.de). This author acknowledges financial support from the German Research Foundation (DFG) within the Cluster of Excellence in Simulation Technology (EXC 310/1) at the University of Stuttgart and the Baden-Württemberg Stiftung gGmbH.

§CEREMADE, Université Paris-Dauphine, France (julien.salomon@dauphine.fr).

options with the Black–Scholes model by primal-dual finite elements and to [12, 16, 34] for an abstract framework on the theory of constrained variational problems.

We are interested in providing fast numerical algorithms to accurately solve the variational equality and inequality systems associated with European and American call and put options for a large variety of different parameter values such as, e.g., interest rate, dividend, and correlation. Availability of such rapid and well-approximating models allows us to solve many-query or real-time scenarios. Many-query tasks under parameter variation arise by statistical investigation, optimization, calibration, or more general parameter identification tasks. Reduced basis (RB) methods are an appropriate means for model reduction and obtaining such accurate and rapid reduced models for standard parametrized parabolic PDEs; cf. [6, 18, 20, 43, 47] and the references therein. These techniques are based on low-dimensional approximation spaces that are constructed by greedy procedures. Convergence behavior is known in some cases [6, 19]. The computational advantage of RB methods over standard discretization methods is obtained by its possible offline/online decomposition: First, a typically expensive offline phase involving the computation of the reduced spaces is performed. This phase only needs to be precomputed once. Then the online phase allows an extremely fast computation of the RB solutions for many new parameters as only low-dimensional systems need to be solved. Recently, we adopted the RB methodology to constrained stationary elliptic problems [22], which we extend here to the instationary case.

We refer the reader to the recent contribution [8] for a tailored RB approach in option pricing with diffusion and jump-diffusion models, which later was generalized to basket options [39] and, in fact, was shown to be a variant of a proper orthogonal decomposition method (POD) [40]. In [37] the use of RB methods to price European options in the Heston model with parameter functions as an initial condition was shown. The application of the RB method can also be extended to the calibration of option pricing models, e.g., [38, 44]. In contrast to our setting, no inequality constraints are taken into account there. Further work relevant for RB methods and variational inequalities comprises [14, 15], which address a time-space formulation of the problem and corresponding analysis. Also, recently, the work has been presented in [52], which alternatively treats the inequality constraints by a primal-dual technique.

One main challenge in our problem setting is the construction of a suitable low-dimensional approximation of the dual cone required for the treatment of the constraints. In this work, we present an algorithm to overcome this difficulty which is based on the greedy procedure and tries to capture as much "volume" as possible in the construction of the dual cone. This is obtained by iteratively selecting snapshots maximizing the angle to the current space. Additionally, we provide some analytical results on a posteriori error control.

Let us briefly relate the current presentation to our previous work. In contrast to [22], which dealt with RB methods for stationary variational inequalities, we treat here instationary problems. Compared to [22], the a posteriori error estimator is also improved. In [23], we presented an RB procedure for American option pricing with a Black–Scholes model and gave first simple examples. The current presentation considerably extends this by including the Heston model and both European and American options and providing an analysis for the corresponding RB scheme. Despite our academic model problems, the approach can be viewed as an interesting and promising technique for future applications in quantitative finance.

The content of this paper is structured as follows: In section 2, we present both a strong

and a variational formulation of European and American option pricing with the Black–Scholes and Heston models. In section 3, an RB method is introduced together with the construction of the primal and dual RB spaces. Section 4 contains the a posteriori error analysis induced by the method and derived from equality and inequality residuals. The implementational aspects of the RB method together with the construction of RB spaces are presented in section 5. Numerical results, given in section 6, illustrate the performance of the method for pricing options in one-dimensional Black–Scholes and two-dimensional Heston models.

2. Variational formulations for European and American options.

2.1. Option pricing models. In this section, we give a brief introduction to the theory of option pricing. An option is a contract which permits its owner the right to buy or sell an underlying asset (a stock or a parcel of shares) at a prespecified fixed strike price $K \geq 0$ before or at a certain time $T \geq 0$, called maturity. There are two basic types of options: a *call* option, which gives a holder a right to buy, and a *put* option, which allows an owner to sell an underlying asset [1, 28]. Also one distinguishes between European options, where exercise is only permitted at maturity T, and American options, which can be exercised at any time before an expiration time T. We will denote the price of the underlying asset by $S = S_\tau \in \mathbb{R}_+$, where $\tau \geq 0$ is the time to maturity T.

In standard option pricing models, e.g., the Black–Scholes model [1, 3, 28], a price of the underlying asset S_τ follows a stochastic process, governed by the stochastic differential equation

$$dS_\tau = \iota S_\tau dt + \sigma_\tau S_\tau dW_\tau, \tag{2.1}$$

with a Wiener process W_τ, a drift ι, and a volatility $\sigma_\tau > 0$. One of the main limitations of these models is the assumption that the volatility of the return on the underlying asset is constant $\sigma_\tau = \sigma$, while in financial markets, the volatility is not a constant, but rather a stochastic variable. The Heston stochastic volatility model [25] takes into account the randomness of the volatility and is based on the following stock price and variance dynamics:

$$dS_\tau = \iota S_\tau dt + \sqrt{v_\tau} S_\tau dW_\tau^1, \tag{2.2}$$

$$dv_\tau = \kappa(\gamma - v_\tau)d\tau + \xi\sqrt{v_\tau} dW_\tau^2, \tag{2.3}$$

where $v_\tau = \sigma^2$ follows a square root process (known as a Cox–Ingersoll–Ross (CIR) process) with the mean variance $\gamma > 0$, rate of mean reversion $\kappa > 0$, and so-called volatility of volatility $\xi > 0$. The Wiener processes W_τ^1 and W_τ^2 are correlated with the correlation parameter $\rho \in [-1, 1]$.

With the use of Ito's formula [28], each model can be formulated in terms of a PDE. For purposes of brevity, we omit the derivation of the equations. The reader is referred to [1, 25, 26] for further details.

We define the spatial differential operators corresponding to the Black–Scholes and Heston models as follows:

$$\mathcal{L}^{BS} P := \frac{1}{2}\sigma^2 S^2 \partial_{SS} P + rS\partial_S P - (r - q)P, \tag{2.4}$$

$$\mathcal{L}^{H} P := \frac{1}{2}\xi^2 v \partial_{vv} P + \rho\xi v S \partial_{vS} P + \frac{1}{2} v S^2 \partial_{SS} P + \kappa(\gamma - v)\partial_v P + rS\partial_S P - rP, \tag{2.5}$$

where r is the interest rate and q is the dividend payment. Then the value of an option $P(\tau, S)$ in the Black–Scholes model and $P(\tau, v, S)$ in the Heston model paying $P_0(S)$ at maturity time T must satisfy the PDE

$$\partial_\tau P + \mathcal{L}P = 0, \tag{2.6}$$

where the value $P_0(S)$ is called a payoff function and $\mathcal{L} := \mathcal{L}^s$, $s = \{BS, H\}$ for the Black–Scholes and the Heston model, respectively.

Remark 1. Assuming a constant volatility in the Heston model and no dividend payment in the Black–Scholes model, $q = 0$, we have $v = \gamma$ and $\xi = 0$, and the Heston equation reduces to the Black–Scholes equation with the constant volatility $\sigma = \sqrt{v}$.

For further derivation of the weak formulation of problem (2.6), we introduce the following notation. Let $\Omega \subset \mathbb{R}^d$, $d = 1, 2$, be a bounded open domain with Lipschitz continuous boundary $\partial\Omega$. We consider $d = 1$ for the Black–Scholes model and $d = 2$ for the Heston model. Note that this is not a limitation for the RB approach that we present. Higher-dimensional problems can readily be treated, as soon as suitable solvers for the discretized PDE are available. We introduce the following functional space:

$$V := \left\{\phi \in H^1(\Omega) : \quad \phi = 0 \ \text{ on } \partial\Omega_D\right\}, \tag{2.7}$$

where $\partial\Omega_D$ denotes a Dirichlet part of the boundary $\partial\Omega$. Further $\langle\cdot,\cdot\rangle_V$ and $\|\cdot\|_V$ denote an inner product and norm on V, similar for other spaces. In the error analysis, we make use of a norm bound; i.e., we denote by C_Ω a constant that satisfies the following for any $v \in V$:

$$\|v\|_{L^2(\Omega)} \le C_\Omega \|v\|_V. \tag{2.8}$$

In the experiments, we use H^1 or weighted H^1 norms for V, but for the sake of generality of our analysis, we introduce this generic constant that includes other frameworks, e.g., the H^1_0 norm for which C_Ω is the Friedrichs–Poincaré constant.

We define a backward time variable $t := T - \tau$ which we will use throughout the paper. This transforms the PDE (2.6) into a standard forward evolution problem. We denote by $(\cdot)_+ := \max(0, \cdot)$, by "$\circ$" the Hadamard product, and we introduce a parameter $\mu \in \mathcal{P} \subset \mathbb{R}^p$, $p = 3, 5$, which parametrizes (2.6). We set $\mu := (\sigma, q, r)$ for the Black–Scholes model and $\mu := (\xi, \rho, \gamma, \kappa, r)$ for the Heston model. But other parameter spaces can be handled as well.

2.2. Pricing of European options. We start our consideration with the simplest case of pricing the European type of option. Since puts and calls of the European option can be easily interchanged via a put-call parity relation [28, p. 163], it suffices for us to consider, e.g., only call options. In addition, there exists a semiclosed analytical solution for these options in the Black–Scholes and Heston models. However, while the Black–Scholes formula [3] provides almost the exact value as that of the European option, the Heston semianalytical formula [25] requires some numerical techniques to approximate the integral. Thus, it is more interesting to consider the case of the Heston model. Then the value of a European call option $P(t, v, S)$, $(v, S) \in \mathbb{R}^2_+$ (the relation to Ω will be given later on) satisfies the linear equation

$$\partial_t P - \mathcal{L}^H P = 0, \qquad t \in (0, T], \tag{2.9}$$

involving partial derivatives and being subject to initial and boundary conditions

$$
\begin{aligned}
&P(0,v,S) = (S-K)_+, && \lim_{S\to 0} P(t,v,S) = 0,\\
&\lim_{S\to+\infty} \partial_S P(t,v,S) = 1, && \lim_{v\to+\infty} P(t,v,S) = S,\\
&rP(t,0,S) = rS\partial_S P(t,0,S) + \kappa\gamma\partial_v P(t,0,S) + \partial_t P(t,0,S). && \text{(2.10)}
\end{aligned}
$$

The description of the boundary conditions can be interpreted as follows: For a large stock price S, we use a Neumann boundary condition which establishes a linear growth of an option price. When the volatility v is 0, we cannot impose any boundary conditions and assume that (2.9) is satisfied on the line $v = 0$. When the stock price is worthless, i.e., $S = 0$, it is natural to assume that the value of the call is also worthless. The option price is increasing with the volatility, but it remains bounded by the stock price; hence when the volatility v is large, we assume the value of the option tends to reach the value of the stock price S. Note that this is not the only way to prescribe boundary conditions for the problem; other types of boundary conditions can be found, e.g., in [9, 11, 53].

Remark 2. The variance process (2.3) is strictly positive if the condition on the parameters $\xi^2 < 2\kappa\gamma$ is satisfied, which is often referred to as the Feller condition; see, e.g., [32]. This condition plays a crucial role in the calibration process of the Heston model, and it is uncommon that the parameters violate it. Thus we restrict ourselves to the choice of model parameters, such that the Feller condition is fulfilled.

Since the operator $\mathcal{L}^H$ in (2.5) is a degenerate parabolic differential operator, the standard way to eliminate the variable coefficient S is to perform the log-transformation of S by introducing a new variable $x := \log\left(\frac{S}{K}\right)$ [35, 49]. Then we are looking for the solution $w(t,v,x) := P(t,v,\log(\frac{S}{K}))$, with the initial condition $w^0(x) := w(0,v,x) = (Ke^x - K)_+$, which satisfies the transformed Heston equation

$$
\partial_t w - L^H w = 0 \tag{2.11}
$$

for all $(v,x) \in \mathbb{R}_+ \times (-\infty,+\infty)$. The operator L^H corresponds to the operator $\mathcal{L}^H$ in (2.5) with respect to a change of variables and is defined as

$$
L^H w := \nabla \cdot A\nabla w - b\cdot\nabla w - rw, \tag{2.12}
$$

with

$$
A := \frac{1}{2}v\begin{bmatrix}\xi^2 & \rho\xi\\ \rho\xi & 1\end{bmatrix}, \qquad b := \begin{bmatrix}-\kappa(\gamma - v) + \frac{1}{2}\xi^2\\ -r + \frac{1}{2}v + \frac{1}{2}\xi\rho\end{bmatrix} \tag{2.13}
$$

and first order spatial differential operator $\nabla := (\partial_v, \partial_x)^T$.

To perform a numerical simulation, we localize the problem (2.11) to a bounded computational domain $\Omega = (v_{\min}, v_{\max}) \times (x_{\min}, x_{\max}) \subset \mathbb{R}^2$ with the variance $v_{\min} > 0$. Then the

boundary conditions transform into

$$\begin{aligned}
&\Gamma_1 : v = v_{min}, && w(t, v_{min}, x) = Ke^x \Phi(d_+) - Ke^{-rt}\Phi(d_-),\\
&\Gamma_2 : v = v_{max}, && w(t, v_{max}, x) = Ke^x,\\
&\Gamma_3 : x = x_{min}, && w = \lambda w(t, v_{max}, x_{min}) + (1-\lambda) w(t, v_{min}, x_{min}),\\
& && \lambda = \frac{v - v_{min}}{v_{max} - v_{min}},\\
&\Gamma_4 : x = x_{max}, && A\frac{\partial w}{\partial \overline{n}}(t, v, x_{max}) = \frac{1}{2} v K e^x,
\end{aligned}$$

with $\overline{n}$ being an outward normal vector at the boundary, $\sigma = \sqrt{v}$, and $d_\pm$ and a cumulative distribution function $\Phi(x)$ defined as

$$d_\pm = \frac{x + (r \pm \frac{\sigma^2}{2})t}{\sigma\sqrt{t}}, \quad \Phi(x) = \frac{1}{\sqrt{2\pi}} \int_{-\infty}^{x} e^{-\frac{z^2}{2}} dz.$$

Using the test function $\phi \in V$ yields the following weak formulation of (2.11):

$$\langle \partial_t w, \phi \rangle_{L^2(\Omega)} + a^H(w, \phi; \mu) = f^E(\phi; \mu) \quad \forall \phi \in V, \tag{2.14}$$

where

$$a^H(w, \phi; \mu) := \langle A\nabla w, \nabla \phi \rangle_{L^2(\Omega)} + \langle b \cdot \nabla w, \phi \rangle_{L^2(\Omega)} + r \langle w, \phi \rangle_{L^2(\Omega)}, \tag{2.15}$$

$$f^E(\phi; \mu) := \left\langle A\frac{\partial w}{\partial \overline{n}}, \phi \right\rangle_{L^2(\Gamma_4)}. \tag{2.16}$$

Various methods can be applied to solve this problem numerically, e.g., [31, 32, 49].

2.3. Pricing of American options. We extend our considerations to American options based on the Black–Scholes and Heston models, for which, in general, a closed form solution does not exist. Since American calls are equal to European calls on nondividend paying stocks [28, p. 159], we will focus only on American put options in both models. Following the same arguments as in section 2.2, we consider the price of the American put in the log-transformed variable $w(x) := P(Ke^x)$ with a log-transformed payoff $w^0(x) := (K - Ke^x)_+$ which solves the following problem:

$$\partial_t w - Lw \geq 0, \qquad w - w^0 \geq 0, \tag{2.17}$$

$$(\partial_t w - Lw) \cdot \left(w - w^0\right) = 0. \tag{2.18}$$

The operator $L := L^s$, $s = \{BS, H\}$ for the Black–Scholes or Heston model, where

$$L^{BS} w := \frac{1}{2}\sigma^2 \partial_{xx}^2 w + (r - q)\partial_x w - rw. \tag{2.19}$$

The boundary conditions for the Heston model are set to $w = w^0(x)$ on $\partial\Omega_D := \Gamma_1 \cup \Gamma_3 \cup \Gamma_4$ and $\frac{\partial w}{\partial \overline{n}} = 0$ on Γ_2. For the Black–Scholes model, we define $\partial\Omega_D := \{x_{\min}, x_{\max}\}$, and on this boundary we prescribe $w = w^0(x)$.

Our aim is to reformulate the system (2.17)–(2.18) in a variational saddle point form [33]. Define $W := V'$ to be the dual space of V and $M \subset W$ to be a dual cone. For all $\eta \in W$, $v \in V$ introduce a duality pairing $b : W \times V \to \mathbb{R}$, $b(\eta, v) = \langle \eta, v \rangle_{V',V}$ and $\widetilde{g}(\eta) := b(\eta, w^0)$. The bilinear form of the Black–Scholes equation reads

$$a^{BS}(w, \phi; \mu) := \frac{1}{2}\sigma^2 \langle \partial_x w, \partial_x \phi \rangle_{L^2(\Omega)} - (r-q)\langle \partial_x w, \phi \rangle_{L^2(\Omega)} + r\langle w, \phi \rangle_{L^2(\Omega)}. \tag{2.20}$$

To treat the problem numerically, we use a θ-scheme for the discretization in time and conforming piecewise linear finite elements for the discretization in spatial direction. We divide $(0, T]$ into L subintervals of equal length $\Delta t := \frac{T}{L}$ and define $w^n := w(t^n, v, x) \in H^1(\Omega)$, $t^n := n\Delta t$, $0 < n \leq L$. In order to ensure Dirichlet boundary conditions, we set $w^n = u^n + u_g^n$, where $u^n := u(t^n, \cdot, \cdot) \in V$ solves (2.17)–(2.18) with homogeneous Dirichlet boundary conditions, and $u_g^n := u_g(t^n, \cdot, \cdot) \in H^1(\Omega)$ is a Dirichlet lift function, which extends nonhomogeneous boundary conditions to the interior of the domain. For $0 < n \leq L-1$, we introduce the operators

$$f^n(\phi; \mu) := -\left\langle \frac{u_g^{n+1} - u_g^n}{\Delta t}, \phi \right\rangle_{L^2(\Omega)} - a(\theta u_g^{n+1} + (1-\theta)u_g^n, \phi; \mu), \tag{2.21}$$

$$g^n(\eta - \lambda^{n+1}; \mu) := \widetilde{g}(\eta - \lambda^{n+1}; \mu) - b(\eta - \lambda^{n+1}, u_g^{n+1}), \tag{2.22}$$

and the discrete problem in saddle point form reads as follows.

Definition 2.1 (detailed problem). *For $\mu \in \mathcal{P}$ and given initial data $u^0 \in V$ find $(u^{n+1}(\mu), \lambda^{n+1}(\mu)) \in V \times M$ for $0 < n \leq L-1$ and $\phi \in V, \eta \in M$ satisfying*

$$\left\langle \frac{u^{n+1} - u^n}{\Delta t}, \phi \right\rangle_{L^2(\Omega)} + a(\theta u^{n+1} + (1-\theta)u^n, \phi; \mu) - b(\lambda^{n+1}, \phi) = f^n(\phi; \mu), \tag{2.23}$$

$$b(\eta - \lambda^{n+1}, u^{n+1}) \geq g^n(\eta - \lambda^{n+1}; \mu). \tag{2.24}$$

The bilinear form $a(\cdot, \cdot; \mu) := a^s(\cdot, \cdot; \mu)$, $s = \{BS, H\}$, is specified for each model in (2.20) or (2.15). Here and in the following, we frequently omit the argument μ whenever the parameter value is clear from the context. The problem (2.23)–(2.24) can be considered as a model-independent formulation for pricing American put options. Moreover, the European call option is also enclosed in this formulation by the exchange of $f^n(\cdot; \mu)$ with $f^n(\cdot; \mu) + f^E(\cdot; \mu)$, initial conditions, and omitting $b(\cdot, \cdot)$ and $g^n(\cdot, \mu)$ terms. Therefore, in further discussions of the implementation aspects and analysis, we will focus only on the general American put option case, and we will not distinguish the models used to price the option. However, in section 6, we present and compare numerical results for European and American options in both models.

By a generalized Lax–Milgram argument, a problem of type (2.23)–(2.24) is well-posed if the bilinear form $a(\cdot, \cdot, \mu)$ is continuous and coercive, $f^n(\cdot, \mu)$, $g^n(\cdot; \mu)$ are linear and continuous, and $b(\cdot, \cdot)$ is inf-sup stable. In particular, for the Heston model, if $v \geq v_{\min} > 0$, the matrix A in (2.13) is positive definite on $\overline{\Omega}$, and under the suitable relation on the coefficients, we obtain the coercivity and continuity of $a(\cdot, \cdot; \mu)$. This issue for the European call option was studied in great detail in [49]. The well-posedness of the problem in the Black–Scholes

settings can be found, e.g., in [1, Chap. 6]. The coercivity, continuity, and inf-sup constants are defined as follows:

$$\alpha_a(\mu) := \inf_{u\in V} \frac{a(u,u;\mu)}{\|u\|_V^2} > 0, \qquad \gamma_a(\mu) := \sup_{u\in V}\sup_{v\in V} \frac{a(u,v;\mu)}{\|u\|_V\|v\|_V} < \infty \quad \forall \mu \in \mathcal{P}, \tag{2.25}$$

$$\beta := \inf_{\eta\in W}\sup_{v\in V} \frac{b(\eta,v)}{\|\eta\|_W\|v\|_V} > 0. \tag{2.26}$$

Also, for our choice of a dual space and cone we assume

$$\langle \eta, \eta' \rangle_W \geq 0 \quad \forall \eta, \eta' \in M. \tag{2.27}$$

3. Reduced basis setting.

In this section, we provide the RB scheme for the variational inequality problem and present the main analytical results.

3.1. Reduced basis discretization.

Standard finite element approaches do not exploit the structure of the solution manifold under parameter variation, and for a given parameter value, a high-dimensional system has to be solved. In what follows, we introduce a specific Galerkin approximation of the solution, based on the RB method. The central step of the RB method mainly consists in computing parametric solutions in low-dimensional subspaces of V and W, defined in section 2, that are generated with particular solutions, the so-called *snapshots*, of our problem.

Let us explain the corresponding formulation in more detail. For $N \in \mathbb{N}$, consider a finite subset $\mathcal{P}_N := \{\mu_1, \dots, \mu_N\} \subset \mathcal{P}$ with $\mu_i \neq \mu_j \ \forall i \neq j$. The reduced spaces V_N and W_N are defined by $V_N := \operatorname{span}\{\psi_1, \dots, \psi_{N_V}\}$ and $W_N := \operatorname{span}\{\xi_1, \dots, \xi_{N_W}\}$, where $\psi_i \in V$ and $\xi_i \in M$ are suitably constructed from the large set of snapshot solutions $u^n(\mu_i)$, $i = 1, \dots, N$, $n = 0, \dots, L$, and $\lambda^n(\mu_i)$, $i = 1, \dots, N$, $n = 1, \dots, L$, and the reduced dimensions N_V, N_W are preferably small. Both families $\Psi_N = (\psi_j)_{j=1,\dots,N_V}$ and $\Xi_N = (\xi_j)_{j=1,\dots,N_W}$ are supposed to be composed of linearly independent functions, and hence are so-called *reduced bases*. Numerical algorithms to build these two sets will be presented in section 5.4. We define the reduced cone as

$$M_N = \left\{ \sum_{j=1}^{N_W} \alpha_j \xi_j, \ \alpha_j \geq 0 \right\},$$

which satisfies $M_N \subseteq M$ due to the assumption of $\xi_i \in M$. In this setting, the reduced problem reads as follows.

Definition 3.1 (reduced problem). *Given $\mu \in \mathcal{P}$, find $u_N^{n+1}(\mu) \in V_N$ and $\lambda_N^{n+1}(\mu) \in M_N$ for $0 \leq n \leq L-1$ that satisfy*

$$\left\langle \frac{u_N^{n+1} - u_N^n}{\Delta t}, v_N \right\rangle_{L^2(\Omega)} + a(\theta u_N^{n+1} + (1-\theta)u_N^n, v_N; \mu) - b(\lambda_N^{n+1}, v_N) = f^n(v_N;\mu), \tag{3.1}$$

$$b(\eta_N - \lambda_N^{n+1}, u_N^{n+1}) \geq g^n(\eta_N - \lambda_N^{n+1}; \mu) \tag{3.2}$$

for all $v_N \in V_N, \eta_N \in M_N$, and the initial value u_N^0 is chosen as an orthogonal projection of u^0 on V_N, i.e., $\langle u_N^0 - u^0, v_N\rangle_V = 0$ for all $v_N \in V_N$.

3.2. Existence, uniqueness, and reproduction property. By the construction procedure for V_N, W_N in section 5, we will assure inf-sup stability of $b(\cdot,\cdot)$ on $W_N \times V_N$ and guarantee that $\beta_N \geq \beta > 0$, where

$$\beta_N := \inf_{\eta_N \in W_N} \sup_{v_N \in V_N} \frac{b(\eta_N, v_N)}{\|\eta_N\|_{W_N} \|v_N\|_{V_N}}, \tag{3.3}$$

which implies the well-posedness of our reduced problem (3.1)–(3.2) with identical arguments as for the detailed saddle point problem. Hence, we ensure existence and uniqueness of the reduced solution. For the details of the proof, we refer the reader to [5, 22, 43]. A further useful property is a basic consistency argument, the reproduction of solutions.

Lemma 3.2 (reproduction of solutions). *If for some μ it holds that $u^{n+1}(\mu) \in V_N$ and $\lambda^{n+1}(\mu) \in M_N$ for $0 < n \leq L-1$ and $u^0(\mu) \in V_N$, then*

$$u_N^{n+1}(\mu) = u^{n+1}(\mu), \quad \lambda_N^{n+1}(\mu) = \lambda^{n+1}(\mu) \quad \forall n = 1, \dots, L-1.$$

Proof. We prove this property by induction. For $n = 0$, $u^0 \in V_N$ and for $u_N^0 \in V_N$ we have $\langle u_N^0 - u^0, v_N \rangle_V = 0$ for all $v_N \in V_N$. Set $v_N = u_N^0 - u^0$. Then

$$\langle u_N^0 - u^0, u_N^0 - u^0 \rangle_V = 0,$$

which is true only for $u_N^0 = u^0$. For the induction step, we assume that $u^n = u_N^n$, $\lambda^n = \lambda_N^n$. Then, choosing $v = v_N \in V_N \subset V$, $\eta = \eta_N \in M_N \subset M$, we directly obtain

$$\begin{aligned} &\left\langle \frac{u^{n+1} - u_N^n}{\Delta t}, v_N \right\rangle_{L^2(\Omega)} + a(\theta u^{n+1} + (1-\theta) u_N^n, v_N; \mu) - b(\lambda^{n+1}, v_N) = f^n(v_N; \mu), \\ &b(\eta_N - \lambda^{n+1}, u^{n+1}) \geq g^n(\eta_N - \lambda^{n+1}; \mu), \end{aligned}$$

which implies that $(u^{n+1}, \lambda^{n+1}) \in V_N \times M_N$ solves the reduced problem (3.1)–(3.2). Due to the uniqueness of the solution, we obtain $u_N^{n+1} = u^{n+1}$ and $\lambda_N^{n+1} = \lambda^{n+1}$. ∎

4. A posteriori error analysis. In this section, we present an a posteriori analysis of our RB scheme. In particular, only the more challenging constraint case of American options is considered; as for the European option model, the well-established standard RB error analysis for linear parabolic problems [18, 17, 13] can be applied, which we omit in this work.

Again, to simplify the presentation, we omit the parameter vector μ in the notation of a, f^n, g^n. In the same way, we only consider the case $\theta = 1$, that is, an implicit Euler time discretization. However, the analysis presented hereafter holds for any $\theta \in [1/2, 1]$, up to technical supplementary computations. For the case $\theta \in [0, 1/2)$, we expect to encounter similar requirements as for the unconstrained θ-scheme, i.e., an inverse estimate to (2.8) and a CFL condition on the time step; cf. [16, 41]. We start by introducing relevant residuals and preliminary results.

4.1. Residuals and preliminary results. In order to evaluate the approximation errors induced by our method, we define, for $n = 0, \dots, L-1$, the equality and inequality residuals

by

$$r^n(v) := \left\langle \frac{u_N^{n+1} - u_N^n}{\Delta t}, v \right\rangle_{L^2(\Omega)} + a(u_N^{n+1}, v) - b(\lambda_N^{n+1}, v) - f^n(v) \qquad \forall v \in V,$$
$$s^n(\eta) := b(\eta, u_N^{n+1}) - g^n(\eta) \qquad \forall \eta \in M.$$

We also introduce the primal and dual errors

$$e_u^n = u_N^n - u^n, \quad e_\lambda^n = \lambda_N^n - \lambda^n. \tag{4.1}$$

Using the linearity of r^n, one finds that

$$r^n(v) = \left\langle \frac{e_u^{n+1} - e_u^n}{\Delta t}, v \right\rangle_{L^2(\Omega)} + a(e_u^{n+1}, v) - b(e_\lambda^{n+1}, v). \tag{4.2}$$

As a consequence of the inf-sup stability, one can bound the dual error by the primal error, as stated in the next lemma.

Lemma 4.1 (primal/dual error relation). *For $n = 0, \dots, L-1$, the dual error at time step t^n can be bounded by the primal error as*

$$\|e_\lambda^{n+1}\|_W \le \frac{1}{\beta} \left(\frac{C_\Omega}{\Delta t} \|e_u^{n+1} - e_u^n\|_{L^2(\Omega)} + \gamma_a \|e_u^{n+1}\|_V + \|r^n\|_{V'} \right). \tag{4.3}$$

Proof. The inf-sup stability of $b(\cdot, \cdot)$ guarantees the existence of a $v^\star \in V, v^\star \neq 0$ such that

$$\beta \|v^\star\|_V \|e_\lambda^{n+1}\|_W \le b(v^\star, e_\lambda^{n+1}).$$

Using (4.2), we find that

$$\begin{aligned} \beta \|v^\star\|_V \|e_\lambda^{n+1}\|_W &\le \left\langle \frac{e_u^{n+1} - e_u^n}{\Delta t}, v^\star \right\rangle_{L^2(\Omega)} + a(e_u^{n+1}, v^\star) - r^n(v^\star) \\ &\le \frac{1}{\Delta t} \|e_u^{n+1} - e_u^n\|_{L^2(\Omega)} \|v^\star\|_{L^2(\Omega)} + \gamma_a \|e_u^{n+1}\|_V \|v^\star\|_V + \|r^n\|_{V'} \|v^\star\|_V, \end{aligned}$$

and the result then follows from (2.8). ∎

4.2. Projectors on the cone. Let us then introduce, for $n = 0, \dots, L-1$, the Riesz representer $\eta_s^n \in W$ of our inequality residual:

$$\langle \eta, \eta_s^n \rangle_W = s^n(\eta), \quad \eta \in W.$$

Contrary to $\|r^n\|_V$, the quantity $\|s^n\|_W = \|\eta_s^n\|_W$ is not a straightforward error estimator component because of the inequality constraint. We obviously would correctly penalize if $s^n(\eta) > 0$ for some $\eta \in M$ as desired, but we would also penalize $s^n(\eta) < 0$, which is not necessary. Hence, we need to cope with the inherent nonlinearity induced by the inequalities. For this purpose, we consider a family of projectors on the cone $\pi^n : W \to M$ which are assumed to satisfy, for $n = 0, \dots, L-1$,

$$\langle \pi^n(\eta_s^n), \lambda_N^{n+1} \rangle_W = 0. \tag{4.4}$$

Having (4.4) and the characterization (2.27) of the dual cone M, we find that

$$\langle e_\lambda^{n+1}, \pi^n(\eta_s^n)\rangle_W = \langle \lambda_N^{n+1} - \lambda^{n+1}, \pi^n(\eta_s^n)\rangle_W = -\langle \lambda^{n+1}, \pi^n(\eta_s^n)\rangle_W \leq 0. \tag{4.5}$$

Remark 3. Projectors satisfying (4.4) improve the one proposed in [22], namely, one term in the error bound can be canceled. We also refer the reader to [48, 51], where such techniques are applied for finite element–based error estimators in contact mechanics and for obstacle problems.

4.3. A posteriori error estimators. We are now in a position to define an a posteriori error estimator associated with our method.

Theorem 4.2. *Define the a posteriori quantities*

$$\delta_s^n = \|\eta_s^n - \pi^n(\eta_s^n)\|_W, \ \ \delta_r^n = \|r^n\|_{V'}.$$

One has

$$\frac{1}{2}\|e_u^L\|^2_{L^2(\Omega)} + \frac{\alpha_a}{2}\Delta t \sum_{n=0}^{L} \|e_u^n\|_V^2 \leq \sum_{n=0}^{L} \frac{1}{2}\left(\frac{C_\Omega \delta_s^n}{\beta}\right)^2 + \Delta t \frac{\delta_s^n \delta_r^n}{\beta} + \frac{\Delta t}{2\alpha_a}\left(\delta_r^n + \frac{\gamma_a \delta_s^n}{\beta}\right)^2 + \frac{1}{2}\|e_u^0\|^2_{L^2(\Omega)}.$$

Proof. First, we note that we have for all $n = 0, \ldots, L-1$

$$s^n(\lambda_N^{n+1}) = 0, \tag{4.6}$$

and we recall that for all $n = 1, \ldots, L$

$$b(\lambda^n, u^n) = g^n(\lambda^n). \tag{4.7}$$

From (4.2), we then have

$$\left\langle \frac{e_u^{n+1} - e_u^n}{\Delta t}, e_u^{n+1} \right\rangle_{L^2(\Omega)} + a(e_u^{n+1}, e_u^{n+1}) = r^n(e_u^{n+1}) + b(e_\lambda^{n+1}, e_u^{n+1}). \tag{4.8}$$

Let us focus on the term $b(e_\lambda^{n+1}, e_u^{n+1})$. Thanks to (4.5), (4.6), (4.7), the definition of s^n, and the fact that $g^n(\lambda_N^{n+1}) - b(\lambda_N^{n+1}, u^{n+1}) \leq 0$ from (2.24), this term can be simplified as follows:

$$\begin{aligned}
b(e_\lambda^{n+1}, e_u^{n+1}) &= b(\lambda_N^{n+1}, u_N^{n+1}) - b(\lambda^{n+1}, u_N^{n+1}) - b(\lambda_N^{n+1}, u^{n+1}) + b(\lambda^{n+1}, u^{n+1}) \\
&\leq g^n(\lambda_N^{n+1}) - s^n(\lambda^{n+1}) - g^n(\lambda^{n+1}) - g^n(\lambda_N^{n+1}) + g^n(\lambda^{n+1}) \\
&= -s^n(\lambda^{n+1}) = s^n(e_\lambda^{n+1}) = \langle e_\lambda^{n+1}, \eta_s^n\rangle_W \\
&= \langle e_\lambda^{n+1}, \pi^n(\eta_s^n)\rangle_W + \langle e_\lambda^{n+1}, \eta_s^n - \pi^n(\eta_s^n)\rangle_W \\
&\leq \|e_\lambda^{n+1}\|_W \|\eta_s^n - \pi^n(\eta_s^n)\|_W = \delta_s^n \|e_\lambda^{n+1}\|_W.
\end{aligned}$$

This estimate combined with (4.8) and the coercivity of a gives rise to

$$\left\langle \frac{e_u^{n+1} - e_u^n}{\Delta t}, e_u^{n+1} \right\rangle_{L^2(\Omega)} + \alpha_a \|e_u^{n+1}\|_V^2 \leq \delta_r^n \|e_u^{n+1}\|_V + \delta_s^n \|e_\lambda^{n+1}\|_W. \tag{4.9}$$

The first term of inequality (4.9) can be expressed as

$$\left\langle \frac{e_u^{n+1}-e_u^n}{\Delta t}, e_u^{n+1} \right\rangle_{L^2(\Omega)} = \frac{1}{2\Delta t}\|e_u^{n+1}\|^2_{L^2(\Omega)} - \frac{1}{2\Delta t}\|e_u^n\|^2_{L^2(\Omega)} + \frac{1}{2\Delta t}\|e_u^{n+1}-e_u^n\|^2_{L^2(\Omega)}. \tag{4.10}$$

Using Lemma 4.1 and Young's inequality, we then bound $\|e_\lambda^{n+1}\|_W$ in (4.9):

$$\delta_s^n\|e_\lambda^{n+1}\|_W \le \frac{1}{2\Delta t}\left(\frac{C_\Omega \delta_s^n}{\beta}\right)^2 + \frac{\delta_s^n\delta_r^n}{\beta} + \frac{1}{2\Delta t}\|e_u^{n+1}-e_u^n\|^2_{L^2(\Omega)} + \frac{\gamma_a\delta_s^n}{\beta}\|e_u^{n+1}\|_V.$$

Combining this estimate with (4.10), we can simplify (4.9) as follows:

$$\frac{1}{2\Delta t}\|e_u^{n+1}\|^2_{L^2(\Omega)} + \alpha_a\|e_u^{n+1}\|_V^2 \le \frac{1}{2\Delta t}\|e_u^n\|^2_{L^2(\Omega)} + \frac{1}{2\Delta t}\left(\frac{C_\Omega\delta_s^n}{\beta}\right)^2 + \frac{\delta_s^n\delta_r^n}{\beta} + \left(\delta_r^n + \frac{\gamma_a\delta_s^n}{\beta}\right)\|e_u^{n+1}\|_V. \tag{4.11}$$

Using Young's inequality gives

$$\left(\delta_r^n + \frac{\gamma_a\delta_s^n}{\beta}\right)\|e_u^{n+1}\|_V \le \frac{1}{2\alpha_a}\left(\delta_r^n + \frac{\gamma_a\delta_s^n}{\beta}\right)^2 + \frac{\alpha_a}{2}\|e_u^{n+1}\|_V^2.$$

We get the result by combining the latter with (4.11), summing the resulting inequalities from $n=0$ up to $L-1$, and multiplying the result by Δt. ∎

5. Implementational aspects.

In this section, we mainly discuss the implementational aspects of solving RB problem (3.1)–(3.2) associated with our detailed formulation (2.23)–(2.24).

5.1. Solution of the detailed problem.

Let us give a few remarks about the solvability of the detailed problem. The differential operator in (2.23) is of convection-diffusion type with constant (in the Black–Scholes model) or variable (in the Heston model) coefficients. Thus, to enhance the quality of the solution for the case when a convective term may dominate the diffusive one, one can use a finer mesh or a different discretization scheme, e.g., a streamline upwind Petrov–Galerkin method [4]. For our numerical simulations, we remain with a standard Galerkin finite element setting with a sufficiently fine mesh.

For the remainder of the paper, V is now a standard conforming piecewise linear finite element space used for the discretization of the variational inequality (2.23)–(2.24). More precisely, consider a triangulation $\mathcal{T}_h$ of Ω, consisting of J simplices K_h^j, $1 \le j \le J$, such that $\overline{\Omega} = \cup_{K_h\in\mathcal{T}_h}\overline{K}_h$. We then use a standard conforming nodal first order finite element space. We define the discrete space $V_h := \{v \in V | v_{|K_h^j} \in \mathbb{P}^1(K_h^j), 1 \le j \le J\}$ of dimension $H_V := H$. For the sake of simplicity, we omit the index h and consider V to be a discrete finite element space. We associate the basis functions $\phi_i \in V$ with its Lagrange node $m_i \in \overline{\Omega}$, i.e., $\phi_i(m_j) = \delta_{ij}, i, j = 1, \dots, H$.

For the discretization of the Lagrange multipliers in $M \subset W$, we use dual basis functions [50]; that is, we consider a dual finite element basis χ_j of $W := V'$, so that $b(\phi_i, \chi_j) = \delta_{ij}$, $i, j = 1, \ldots, H_W = H$. The cone M is defined by $M = \{\sum_{i=1}^{H_W} \eta_i \chi_i,\ \eta_i \geq 0\}$. We define the inner product matrices $\underline{M}^V := (\langle \phi_i, \phi_j \rangle_V)_{i,j=1}^H$ and $\underline{M}^W := (\langle \chi_i, \chi_j \rangle_V)_{i,j=1}^H$, which are used to compute inner products and norms in the a posteriori error bounds. In addition, $\underline{M}^W = (\underline{M}^V)^{-1}$ [21], and with our setting (2.7), $\underline{M}^V$ is an M-matrix, and hence assumption (2.27) is valid.

As these spaces are assumed to be sufficiently accurate a priori, that is, the finite element discretization error is negligible compared to the reduction error, we do not discriminate notationally between the true and the finite element spaces. However, a more extensive analysis also has to take into account the quality of the detailed solution.

5.2. Solution algorithm for the reduced problem. We shall now present a method to solve problem (3.1)–(3.2). The approach we follow is mainly based on the primal-dual active set strategy [24, 27], which is equivalent to a semismooth Newton method; thus a superlinear convergence of the algorithm can be achieved.

We expand the solution $(u_N^n(\mu), \lambda_N^n(\mu))$ of (3.1)–(3.2) as $u_N^n(\mu) = \sum_{j=1}^{N_V} \overline{u}_{N,j}^n \psi_j$ and $\lambda_N^n(\mu) = \sum_{j'=1}^{N_W} \overline{\lambda}_{N,j'}^n \xi_{j'}$ with the coefficient vectors $U_N^n = (\overline{u}_{N,j})_{j=1}^{N_V} \in \mathbb{R}^{N_V}$, $\Lambda_N^n = \left(\overline{\lambda}_{N,j'}\right)_{j'=1}^{N_W} \in \mathbb{R}^{N_W}$. We also introduce the following set of notation: For $\nu \in [-1, 1]$, denote by $\mathcal{M}$, $\mathcal{A}^\nu(\mu)$ and $\mathcal{B}$ the matrices of coefficients $(\mathcal{M})_{i,j} = \langle \psi_i, \psi_j \rangle_V$, $(\mathcal{A}^\nu(\mu))_{i,j} = \langle \psi_i, \psi_j \rangle + \nu \Delta t a(\psi_i, \psi_j; \mu)$, and $(\mathcal{B})_{i,j'} = b(\xi_{j'}, \psi_i)$ with $1 \leq i, j \leq N_V$ and $1 \leq j' \leq N_W$, respectively. Denote also by $\mathcal{F}^n(\mu)$ and $\mathcal{G}^n(\mu)$ the vectors of components $f^n(\psi_i; \mu)$ and $g^n(\xi_{j'}; \mu)$, respectively. Let U and Λ be generic coefficient vectors of length N_V and N_W, respectively; then we introduce the function $\varphi(U, \Lambda) = \Lambda - \max(0, \Lambda - c(\mathcal{B}^T U - \mathcal{G}^n(\mu)))$, where $c > 0$ and $\max(\cdot)$ applies componentwise. With the use of this notation, problem (3.1)–(3.2) can be rewritten in the algebraic form

$$\mathcal{A}^\theta(\mu) U_N^{n+1} - \mathcal{B} \Lambda_N^{n+1} = \mathcal{A}^{\theta-1}(\mu) U_N^n + \mathcal{F}^n(\mu), \tag{5.1}$$

$$\varphi(U_N^{n+1}, \Lambda_N^{n+1}) = 0, \tag{5.2}$$

and the initial data is obtained by solving $\mathcal{M} U_N^0 = \left(\langle u^0, \psi_j \rangle_V\right)_{j=1}^{N_V}$. To employ the the primal-dual active set strategy, we introduce the active and inactive sets

$$A(U, \Lambda) = \left\{ p :\ 1 \leq p \leq N_W,\ \left(\Lambda - c(\mathcal{B}^T U - \mathcal{G}^n(\mu)\right)_p \geq 0 \right\},$$

$$I(U, \Lambda) = \left\{ p :\ 1 \leq p \leq N_W,\ \left(\Lambda - c(\mathcal{B}^T U - \mathcal{G}^n(\mu)\right)_p < 0 \right\},$$

where we have denoted by $(\cdot)_p$ the pth component of a vector. A Newton iteration can then be applied, which gives rise to the next algorithm.

Algorithm 1 (time solver for the reduced system). *Given a tolerance $\varepsilon > 0$ and initial conditions (U_N^0, Λ_N^0), the trajectory (U_N^n, Λ_N^n), $n = 0, \ldots, L$, is computed recursively as follows. Suppose that at time step $t_n = n\Delta t$, (U_N^n, Λ_N^n) is known.*

1. *Set $(U_N^{n+1,0}, \Lambda_N^{n+1,0}) := (U_N^n, \Lambda_N^n)$ and $Tol = +\infty$.*
2. *While $Tol > \varepsilon$, do*

(a) *Define* $(U_N^{n+1,k+1}, \Lambda_N^{n+1,k+1})$ *as the solution of*

$$\begin{aligned}
\mathcal{A}^{\theta}(\mu)U_N^{n+1,k+1} - \mathcal{B}\Lambda_N^{n+1,k+1} &= \mathcal{A}^{\theta-1}(\mu)U_N^{n} + \mathcal{F}^{n}(\mu),\\
\left(\mathcal{B}^T U_N^{n+1,k+1}\right)_p &= \left(\mathcal{G}^n(\mu)\right)_p \qquad \forall p \in A(U_N^{n+1,k}, \Lambda_N^{n+1,k}),\\
\left(\Lambda_N^{n+1,k+1}\right)_p &= 0 \qquad\qquad \forall p \in I(U_N^{n+1,k}, \Lambda_N^{n+1,k}).
\end{aligned}$$

(b) *Set* $Tol = \|U_N^{n+1,k+1} - U_N^{n+1,k}\|_V + \|\Lambda_N^{n+1,k+1} - \Lambda_N^{n+1,k}\|_W$.

3. *Define* $(U_N^{n+1}, \Lambda_N^{n+1}) = (U_N^{n+1,k+1}, \Lambda_N^{n+1,k+1})$.

Note that $U_N^{n+1,k}$ and $\Lambda_N^{n+1,k}$ do not appear in the iteration (except in the definitions of the sets $A(U_N^{n+1,k}, \Lambda_N^{n+1,k})$ and $I(U_N^{n+1,k}, \Lambda_N^{n+1,k})$) as the functions involved in (5.1)–(5.2) are either linear or piecewise linear. Using the previous time-step solution as a start iterate, the active set is already a very good guess, and thus we can expect a good convergence of the Newton method.

5.3. Projectors. For the a posteriori error estimators, we require suitable projectors on the cone. In the case of our finite element basis, we simply choose them by their discrete vectorial representation in the dual finite element space as

$$\pi^n(\eta) := I_{|\{\Lambda_N^{n+1}=0\}} \circ \left([\mathcal{B}^T U - \mathcal{G}^n(\mu)]_+\right),$$

where for $p = 1, \dots, N_w$, $I_{|\{\Lambda_N^{n+1}=0\}}$ is defined by $(I_{|\{\Lambda_N^{n+1}=0\}})_p = 0$ if $(\Lambda_N^{n+1})_p \neq 0$, and $(I_{|\{\Lambda_N^{n+1}=0\}})_p = 1$ else. Given a coefficient vector X, we denote by $[X]_+$ its positive part, that is, $([X]_+)_p = 0$ if $(X)_p \leq 0$ and $([X]_+)_p = (X)_p$ otherwise. With this definition, the property (4.4) is trivially fulfilled.

5.4. Computation of primal and dual reduced basis. In this section, we present a method to build the reduced primal basis $\Psi_N \subset V$ and dual basis $\Xi_N \subset M$. The approach we follow consists in building iteratively and simultaneously the reduced primal and dual basis in a greedy fashion, as presented in Algorithm 2. We consider a finite training set $\mathcal{P}_{train} \subset \mathcal{P}$ small enough such that it can be scanned quickly, but sufficiently large to represent the parameter space well. After a (quite arbitrary) choice of the initial reduced spaces, we proceed in a greedy loop: For a given primal and dual space at stage k, we identify the parameter vector μ_{k+1} in the training set that currently leads to the worst RB approximation. For this parameter, new primal and dual basis vectors are generated, and this loop is repeated $N_{\max} \in \mathbb{N}$ times. To be more precise, the selection of new primal vectors is based on the idea of the POD-Greedy procedure, which meanwhile is standard for RB methods for time-dependent parametric problems [20, 23] and has provable convergence rates [19]. The main step consists in computing the complete simulation of the worst-resolved trajectory, extracting the new information by an orthogonal projection on the current primal space and a compression by a proper orthogonal decomposition (POD) to a single vector, the so-called dominant POD-mode. In the algorithm, $\Pi_{V_N^k}$ denotes the orthogonal projection on V_N^k with respect to $\langle \cdot, \cdot \rangle_V$,

and the dominant POD-mode is given as

$$POD_1\left(\{v^n\}_{n=0}^L\right) := \arg\min_{\|z\|_V=1} \sum_{n=0}^{L} \|v^n - \langle v^n, z\rangle_V z\|_V^2.$$

The new dual basis vectors are selected using an Angle-Greedy argument, which aims at maximizing the volume of the resulting cone [23]. This means that we include the snapshot showing the largest deviation from the current reduced dual space, that is, the vector $\lambda^{n_{k+1}}(\mu_{k+1})$ that maximizes $\measuredangle\left(\lambda^{n_{k+1}}(\mu_{k+1}), W_N^k\right)$, where $\measuredangle(\eta, Y) := \arccos ||\Pi_Y \eta||_W / ||\eta||_W$ denotes the angle between a vector $\eta \in W$ and a linear space $Y \subset W$.

We point out that our system (3.1)–(3.2) has a saddle point structure. Thus ignoring the dual basis in the construction of the primal basis may lead to a reduced system for which the stability cannot be guaranteed. To guarantee the inf-sup stability of our approach, we follow the "inclusion of supremizers" idea introduced first in [42] and later extended in [43] for the Stokes problem. This enrichment consists in including $B\xi_{k+1}$ into the primal space, where $B\xi_{k+1} \in V$ is the solution of $b(\xi_{k+1}, v) = \langle B\xi_{k+1}, v\rangle_V$ for $v \in V$. Then $v = B\xi_{k+1}$ is the element that supremizes the expression $\langle B\xi_{k+1}, v\rangle_V$; hence it is called a "supremizer." This extension ensures that the reduced inf-sup condition (3.3) is satisfied, which can be proven following the lines of [22], and hence the reduced problem is well-posed. We conclude by defining the final reduced space $V_N := \text{span}\Psi_N$ of dimension $N_V := \dim V_N$.

The selection of the "worst" parameter in the greedy loop requires a measure $E(\mu)$, which is an error estimator that can be chosen as one of these three quantities:

$$E_{L^2}^{true}(\mu) = \Delta t \sum_{n=0}^{L} \|e_u^n\|_V^2, \tag{5.3}$$

$$E_{energy}^{true}(\mu) = \frac{1}{2}\|e_u^L\|_{L^2(\Omega)}^2 + \frac{\alpha_a(\mu)}{2}\Delta t \sum_{n=0}^{L} \|e_u^n\|_V^2, \tag{5.4}$$

$$E_{energy}^{Apost}(\mu) = \sum_{n=0}^{L} \frac{1}{2}\left(\frac{C_\Omega \delta_s^n}{\beta}\right)^2 + \Delta t \frac{\delta_s^n \delta_r^n}{\beta} + \frac{\Delta t}{2\alpha_a(\mu)}\left(\delta_r^n + \frac{\gamma_a(\mu)\delta_s^n}{\beta}\right)^2 + \frac{1}{2}\|e_u^0\|_{L^2(\Omega)}^2. \tag{5.5}$$

Hence $E_{L^2}^{true}$ is the squared true L^2-error, E_{energy}^{true} is the true error measured in a space-time energy, and E_{energy}^{Apost} is the a posteriori error bound from the previous section; cf. Theorem 4.2. With this notation, the resulting POD-Angle-Greedy algorithm is fully specified.

Algorithm 2 (POD-Angle-Greedy algorithm). *Given* $N_{\max} > 0$, $\mathcal{P}_{train} \subset \mathcal{P}$

1. *choose arbitrarily* $\mu_1 \in \mathcal{P}_{train}$ *and* $n_1 \in 1, \ldots, L$,
2. *set* $\xi_1 := \lambda^{n_1}(\mu_1)/\|\lambda^{n_1}(\mu_1)\|_W$, $\Xi_N^1 = \{\xi_1\}$, $W_N^1 := \text{span}(\Xi_N^1)$,
3. *set* $\Psi_N^1 := \text{orthonormalize}\{u^{n_1}(\mu_1), B\xi_1\}$, $V_N^1 := \text{span}(\Psi_N^1)$,
4. *for* $k = 1, \ldots, N_{\max} - 1$, *do*
   (a) *define* $\mu_{k+1} := \text{argmax}_{\mu\in\mathcal{P}_{train}}(E(\mu))$,
   (b) *find* $n_{k+1} := \text{argmax}_{n=1,\ldots,L}\left(\measuredangle\left(\lambda^n(\mu_{k+1}), W_N^k\right)\right)$,
   (c) *set* $\xi_{k+1} := \lambda^{n_{k+1}}(\mu_{k+1})/\ \|\lambda^{n_{k+1}}(\mu_{k+1})\|_W$,
   $\Xi_N^{k+1} := \Xi_N^k \cup \{\xi_{k+1}\}$, $W_N^{k+1} := \text{span}(\Xi_N^{k+1})$,

(d) *define* $\tilde{\psi}_{k+1} := POD_1\big(\{u^n(\mu_{k+1}) - \Pi_{V_N^k}(u^n(\mu_{k+1}))\}_{n=0,\dots,L}\big)$,
set $\Psi_N^{k+1} := \text{orthonormalize}\big(\Psi_N^k \cup \{\tilde{\psi}_{k+1}, B\xi_{k+1}\}\big)$, $V_N^{k+1} := \text{span}(\Psi_N^{k+1})$,

5. *define* $\Xi_N := \Xi_N^{N_{\max}}$, $W_N := \text{span}(\Xi_N)$, $N_W := \dim(W_N)$,
6. *define* $\Psi_N := \Psi_N^{N_{\max}}$, $V_N := \text{span}(\Psi_N)$, $N_V := \dim(V_N)$.

Let us give some additional comments on this procedure. First note that the extension steps in the algorithm are only performed if the sets remain linearly independent. Another way of stating this is to say that if a supremizer is already contained in the current space, it will not be inserted again in order to maintain the linear independence of the reduced bases. This results in $|\Psi_N^k| \leq 2k$ and $|\Xi_N^k| \leq k$.

Note also that the orthonormalization steps can be done by either a simple Gram–Schmidt orthonormalization or a singular value decomposition (SVD). In particular the former is very attractive, as V_N^k and $\tilde{\psi}_{k+1}$ are already orthonormal; hence in step 4(d) it is sufficient to orthonormalize the single vector $B\xi_{k+1}$.

Further, we emphasize that the supremizer enrichment in practice also may be skipped. This results in smaller and hence faster reduced models by accepting the loss of a theoretical stability guarantee; see, e.g., [22].

Using the error estimator $E_{energy}^{true}(\mu)$ or $E_{L^2}^{true}(\mu)$ corresponds to working with quantities associated with the true error and is consequently more expensive, as the full trajectories for all parameters in the training set must be precomputed. This is in contrast to the case of working with $E_{energy}^{Apost}(\mu)$, which only involves the reduced solver used in the online phase, and only detailed trajectories for the selected parameters must be computed. Hence, when using $E_{energy}^{Apost}(\mu)$, the training set $\mathcal{P}_{train}$ can be potentially chosen much larger and hence much more representative for the complete parameter domain.

We finally give a short comment on the European option case: In that case, we use the $E_{L^2}^{true}(\mu)$ measure for selecting the worst parameter. Due to the absence of the Lagrange multiplier, we do not obtain a saddle point structure of the problem. Hence, we omit the supremizer enrichment and the Angle-Greedy step, and the algorithm then reduces to the classical (strong) POD-Greedy algorithm.

Remark 4. In addition to the "angle-greedy" strategy used in steps 4(b) and 4(c) of Algorithm 2, alternative algorithms which preserve the positivity can be considered for the construction of the dual reduced bases. As an example one may consider a standard greedy procedure or a nonnegative matrix factorization (NNMF) strategy. NNMF is a part-based representation algorithm which uses the nonnegativity constraints. Originally, the method was applied to face recognition problems [36]. By now different variants of the method exist, such as, e.g., NNMF-orthogonal [7] and NNMF-convolutive [46]. In the context of the RB method, NNMF was recently applied to contact problems [2] and compared to the SVD procedure. We experimentally compared NNMF of different types with angle-greedy and greedy algorithms on an example of American puts for the Heston model. In our application setting, all algorithms performed with similar accuracy. However, the greedy, angle-greedy, and NNMF-convolutive algorithms proved to be the most robust ones. In terms of computational cost, the angle-greedy algorithm is more attractive, and thus we restrict ourselves to it from now on.

6. Numerical results.

6.1. Numerical setting. We start with a description of the numerical values and methods that we consider for the offline solver for the Black–Scholes and Heston models.

We use the θ-scheme presented in section 2 for the time discretization with $\theta = \frac{1}{2}$ for European and $\theta = 1$ for American options. The time domain $[0, T] = [0, 1]$ is discretized with a uniform mesh of step size $\Delta t := T/L$, $L = 20$. The space domain is set to $\Omega = (S_{\min}, S_{\max}) = (0, 300) \subset \mathbb{R}^1$ and $\Omega = (v_{\min}, v_{\max}) \times (x_{\min}, x_{\max}) = (0.0025, 0.5) \times (-5, 5) \subset \mathbb{R}^2$ for the Black–Scholes and Heston models, respectively. The Black–Scholes model is treated in the original S variable, while the Heston model is considered with respect to the log-transformation $x = \log\left(\frac{S}{K}\right)$. As a consequence, we use the H^1 norm for the Heston model and the weighted H^1 norm $u \mapsto \left(\int_\Omega u^2 + S^2(\partial_s u)^2 dS\right)^{1/2}$ for the Black–Scholes model.

For the Black–Scholes model we set $H = 200$ nodes, and for the Heston model $H = 49 \times 97 = 4753$ nodes. To build the basis, we consider a subset $\mathcal{P}_{train}$ of $\mathcal{P}$, which is specified for the Black–Scholes model as in (6.1) and for the Heston model as in (6.2) for European options, and for the Heston model as in (6.3) for American options:

$$\mathcal{P} \equiv [0.0475, 0.0525] \times [0.0014, 0.0016] \times [0.4750, 0.5250] \qquad \subset \mathbb{R}^3, \tag{6.1}$$

$$\mathcal{P} \equiv [0.1, 0.4] \times [0.21, 0.9] \times [0.08, 0.15] \times [1.2, 3] \times [0.01, 0.2] \qquad \subset \mathbb{R}^5, \tag{6.2}$$

$$\mathcal{P} \equiv [0.6, 0.9] \times [0.21, 0.9] \times [0.16, 0.25] \times [3, 5] \times [0.01, 0.2] \qquad \subset \mathbb{R}^5. \tag{6.3}$$

For the Black–Scholes setting, we use $\mathcal{P}_{train}$ composed of 4^3 values chosen equidistantly distributed in $\mathcal{P}$, while for the Heston model the set $\mathcal{P}_{train}$ is varying and specified in every particular case. We define our model parameters $\mu \in \mathcal{P}$ as $\mu \equiv (\rho, q, \sigma)$ and $\mu \equiv (\xi, \rho, \gamma, \kappa, r)$ for the Black–Scholes and Heston models, respectively. The strike K is not considered as a model parameter, since it scales the value of the option. We set $K = 100$ and $K = 1$ for the Black–Scholes and Heston models, respectively. In order to design the reduced primal and dual bases, we use the POD-Angle-Greedy algorithm with different error measures $E(\mu)$.

6.2. European options. We first consider the numerical results and a performance of the RB method for the simpler linear case of the European call option with the Heston model. To illustrate the motivation to apply the RB approach, we demonstrate the variability of the solution in parameter and time. In Figure 1 (top left) the detailed solution for a fixed parameter value at the final time $t = T$ is presented. The evolution of the solution for different time t is shown in Figure 1 (top right) and the variation with respect to parameters in Figure 1 (bottom). After computing the set of snapshots which consists of the detailed solutions for different $\mu_i \in \mathcal{P}_{train}$, we employ the POD-Angle-Greedy algorithm with $E^{true}_{L^2}(\mu)$ as a selection criterion to construct the RB space V_N. As mentioned earlier, this procedure corresponds to the standard strong POD-Greedy algorithm.

We test the RB approach for different dimensions of the parameter domain $\mathcal{P} \subset \mathbb{R}^d$, $d = 2, 3, 5$; namely, we consider $\mu = (\gamma, \kappa) \in \mathbb{R}^2$, $\mu = (\gamma, \kappa, r) \in \mathbb{R}^3$, and $\mu = (\xi, \rho, \gamma, \kappa, r) \in \mathbb{R}^5$. For each choice of μ, the remaining parameter values are assumed to be fixed and taken from the default parameter vector $\mu^* = (0.3, 0.21, 0.095, 2, 0.0198)^T$. In our first test, we consider $\mu = (\kappa, \gamma)$ and $|\mathcal{P}_{train}| = 15^2 = 225$ equidistantly distributed points. The first six orthonormal RB vectors produced by the algorithm are presented in Figure 2.

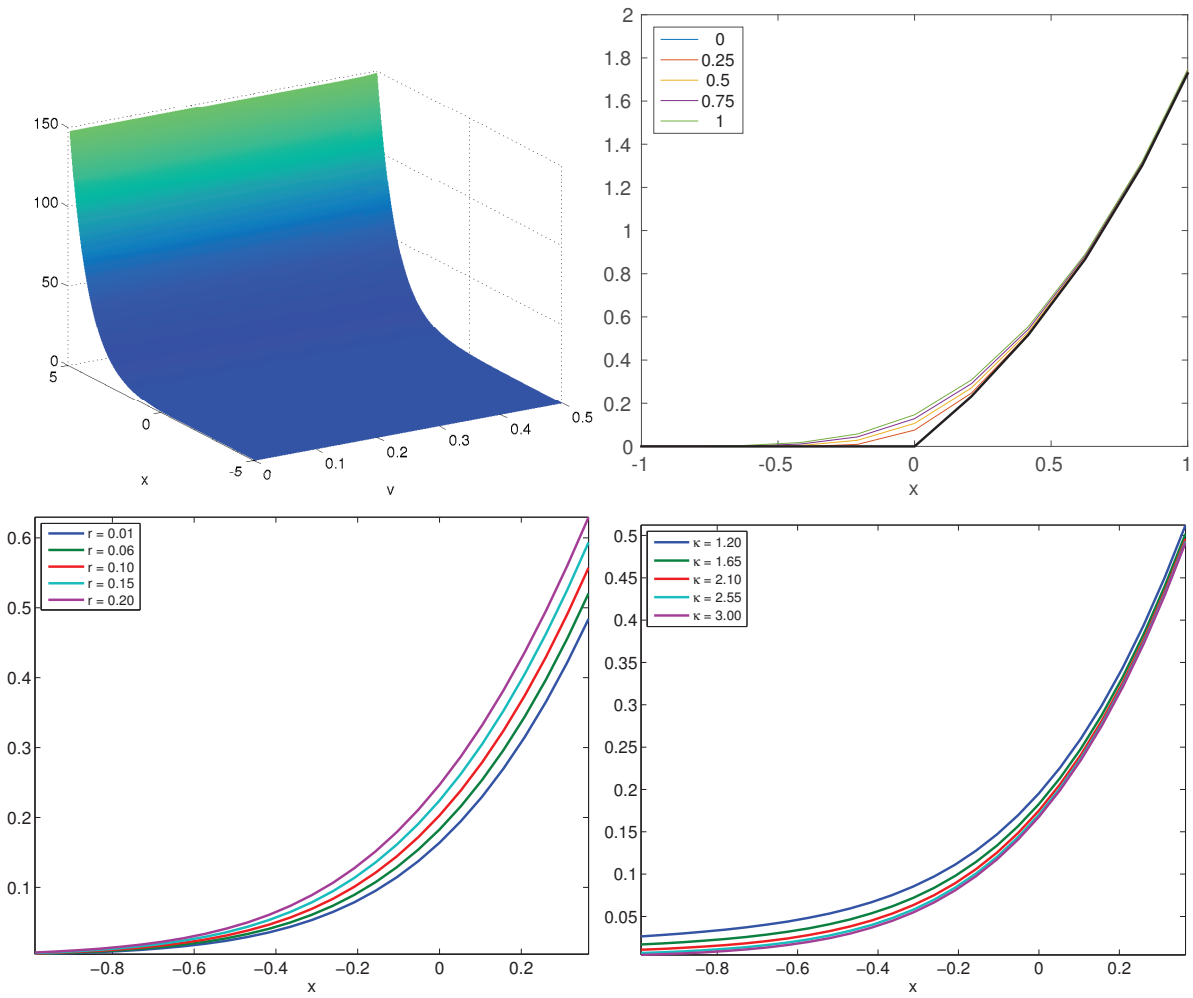

Figure 1. *Top: The value of the European call option with the Heston model for* $\mu = (0.4, 0.55, 0.06, 2.5, 0.0198)^T$ *at* $t = T = 1$ *(left) and a time evolution of the option at* $v = 0.1683$ *(right). Bottom: Snapshots of the solution for different parameter values extracted at a fixed volatility* $v = 0.1683$.

To quantify the efficiency of the RB method, we investigate the error decay when increasing the dimension N_V. For each reduced model, we compute the maximal error $\max_{\mu \in \mathcal{P}_{test}} \left\{ E_{L^2}^{true}(\mu) \right\}$ over a random test set $|\mathcal{P}_{test}| = 400$. In Figure 3, we observe that the error plotted versus the dimension of the reduced model decays exponentially. By the "frequency of the selection" of the parameters in Figure 3 (right), we mean how often the same parameter is chosen during the basis generation. Larger circles indicate training parameters which are chosen more often during the POD-Greedy procedure. The analogous results for other choices of $\mu = (\gamma, \kappa, r)$ and $\mu = (\xi, \rho, \gamma, \kappa, r)$ are presented in Figures 4 and 5. For both cases the exponentially decaying behavior of the error is shown; however, it can be observed that the convergence is slower for larger dimensions of the parameter, which is explained by the increasingly complex parameter dependence of the model. In Figure 5, we also present the evolution of the error

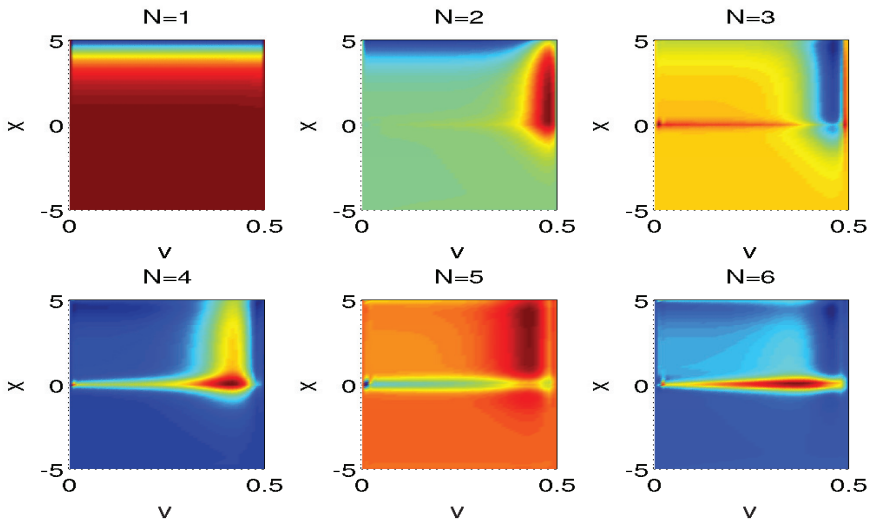

Figure 2. *First six vectors of the reduced basis* $\{\psi_k\}_{k=1}^{N_V} \subset \Psi_N$*, obtained by Algorithm 2 for the European option with the Heston model using* $E(\mu) = E_{L^2}^{true}(\mu)$ *for the case of* $\mu = (\gamma, \kappa)$*.*

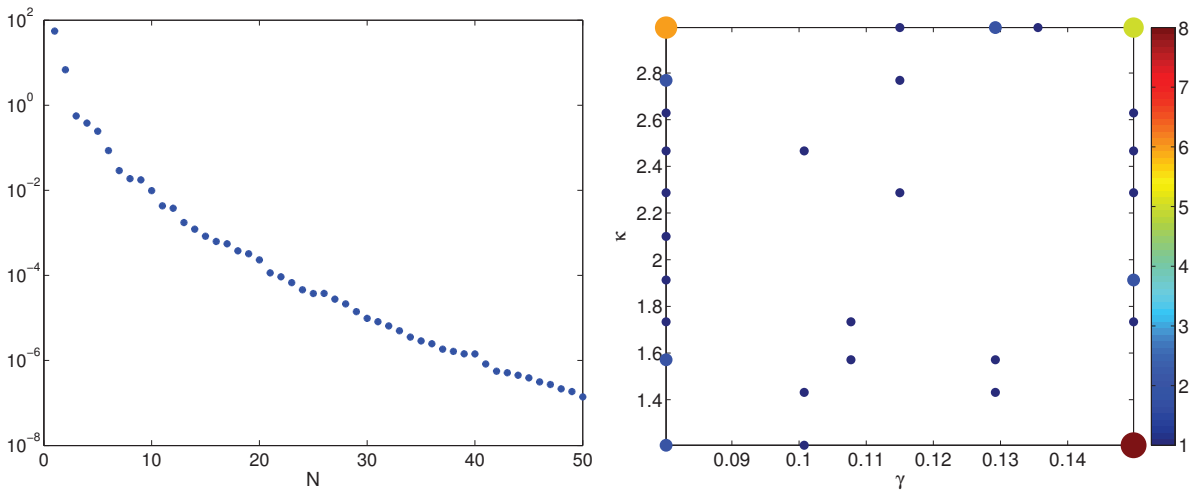

Figure 3. *Left: Evolution of* $\max_{\mu \in \mathcal{P}_{test}} \left\{E_{L^2}^{true}(\mu)\right\}$ *for the European option with the Heston model and* $\mu = (\gamma, \kappa)$*. The test grid is random* $|\mathcal{P}_{test}| = 400$*. Right: Plot of the selected parameters* $\mu_1, \ldots, \mu_N \in \mathcal{P}_{train}$ *and their frequency of the selection in the construction of the reduced basis in Algorithm 2. The train set is composed of* $|\mathcal{P}_{train}| = 15^2 = 225$ *equidistantly distributed points.*

$\max_{\mu \in \mathcal{P}_{train}} \left\{E_{L^2}^{true}(\mu)\right\}$ used for the RB construction in step 4(a) of Algorithm 2.

6.3. American options. In this section, we present the numerical results corresponding to the performance of the RB approach for pricing American options with the Black–Scholes and Heston models and the corresponding a posteriori error estimates.

6.3.1. Examples on the Heston model. For the American option case with the Heston model, we consider the settings of the parameter domain defined in (6.3). For the experiments

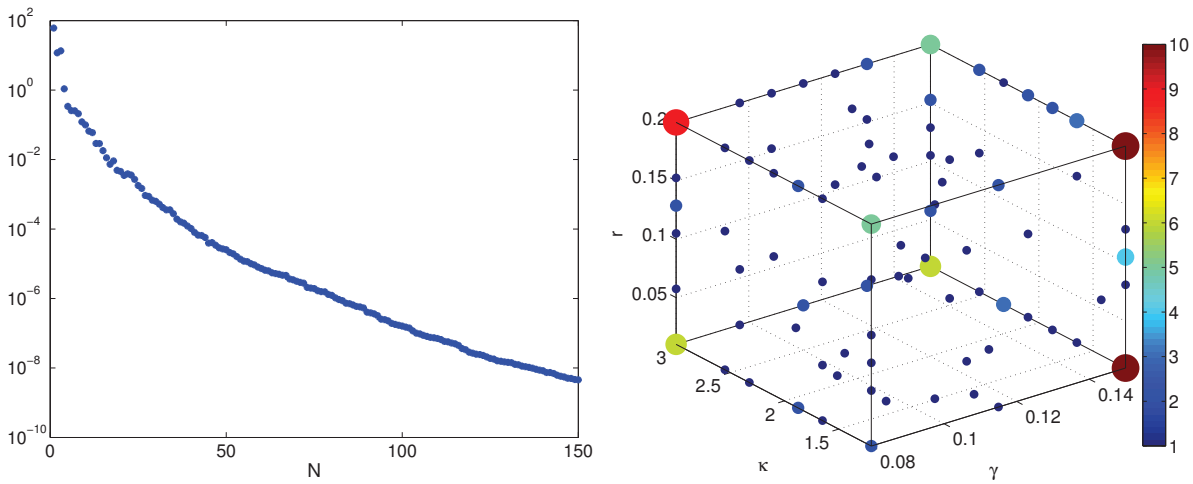

Figure 4. *Left: Evolution of* $\max_{\mu\in\mathcal{P}_{test}}\{E^{true}_{L^2}(\mu)\}$ *for the European call option with the Heston model with* $\mu=(\gamma,\kappa,r)$. *The test grid is random* $|P_{test}|=1024$. *Right: Plot of the selected parameters* $\mu_1,\dots,\mu_N\in\mathcal{P}_{train}$ *and their frequency of the selection in the construction of the reduced basis in Algorithm 2. The train set is composed of* $|\mathcal{P}_{train}|=9^3=729$ *equidistantly distributed points.*

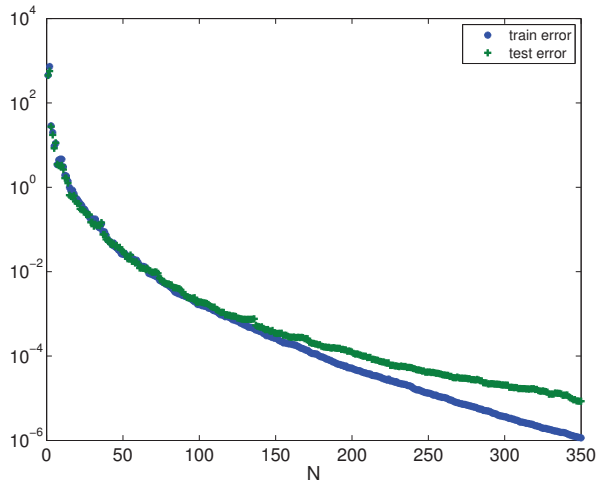

Figure 5. *Left: Evolution of the train error* $\max_{\mu\in\mathcal{P}_{train}}\{E^{true}_{L^2}(\mu)\}$ *(blue stars) and a test error* $\max_{\mu\in\mathcal{P}_{test}}\{E^{true}_{L^2}(\mu)\}$ *(green crosses) for the European call option with the Heston model with* $\mu=(\xi,\rho,\gamma,\kappa,r)$. *The test grid is random* $|P_{test}|=10000$. *The train set composed of* $|\mathcal{P}_{train}|=6^5=7776$ *equidistantly distributed points.*

presented in this section, we consider $\mu\equiv(\gamma,\kappa)$ and, if not stated, the remaining parameter values are set to the corresponding entries of $\mu^*=(0.9,0.21,0.16,3,0.0198)^T$.

The detailed primal solution and a corresponding Lagrange multiplier are presented in Figure 6. In Figure 7, we show the snapshots of the primal solutions and their Lagrange multipliers at different parameter values, which motivates us to apply the RB method to this model. To study the efficiency of the RB approach, we consider the POD-Angle-Greedy

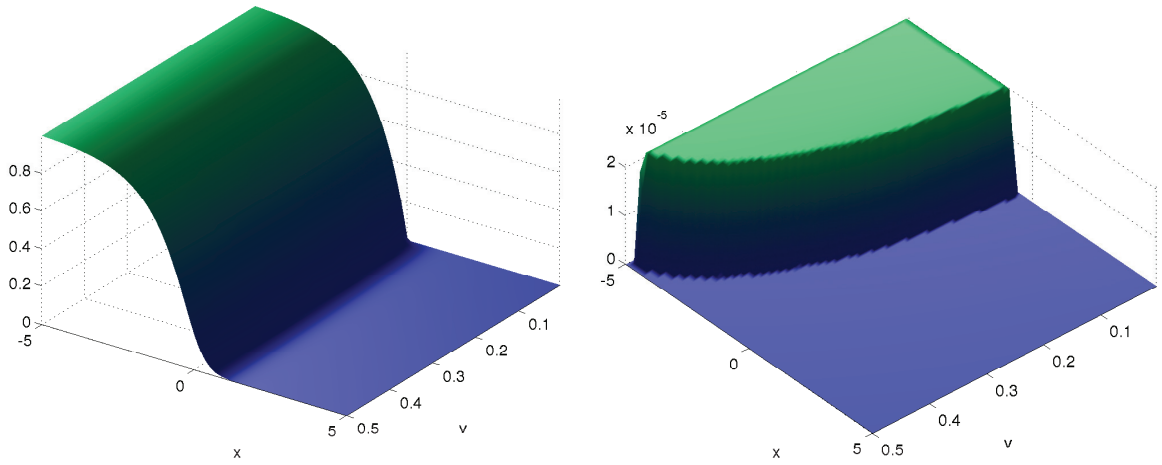

Figure 6. *The solution of the American put with the Heston model for* $\mu = (0.9, 0.21, 0.1750, 3, 0.0198)^T$ *at* $t = T$ *(left) and a corresponding Lagrange multiplier (right).*

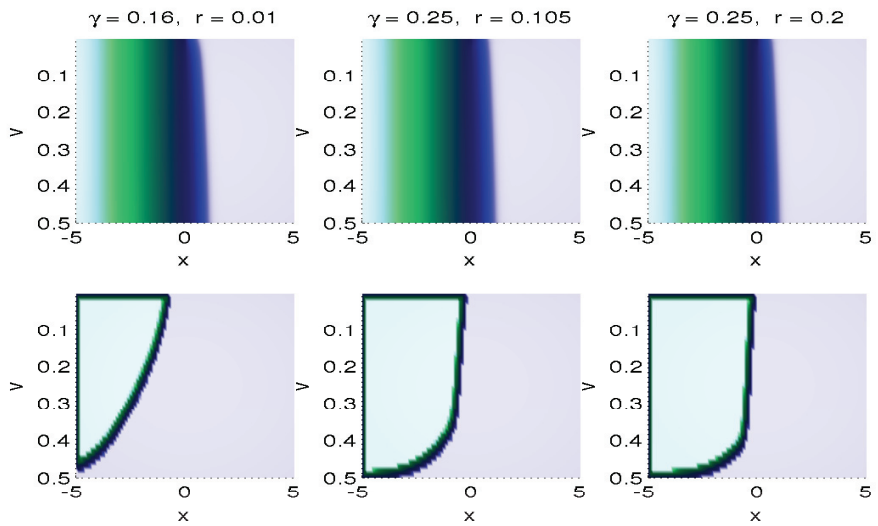

Figure 7. *Top: the primal solutions of the American put option with the Heston model with different values of* γ, r *at the final time* $t = T$ *(top) and corresponding Lagrange multipliers (bottom).*

algorithm with the true error indicator $E(\mu) = E^{true}_{L^2}(\mu)$. We build the hierarchical reduced basis with $N_V = 70$ and $N_W = 35$ using the training set $|\mathcal{P}_{train}| = 7^2 = 49$ uniformly distributed points. The evolution of the error produced by the algorithm is depicted in Figure 8. Each RB model is tested on the random test set $|\mathcal{P}_{test}| = 200$, and the corresponding error $\max_{\mu\in\mathcal{P}_{test}} E^{true}_{L^2}(\mu)$ is also depicted in Figure 8. Similar to the European option case, we observe a good approximation property of the RB method and an exponential convergence of the error.

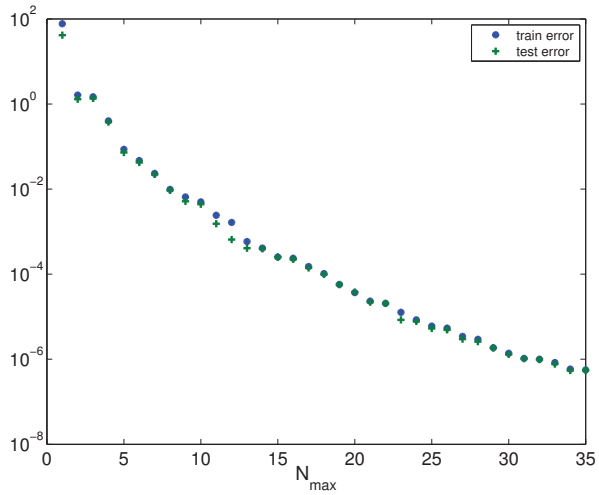

Figure 8. *Evolution of the train error* $\max_{\mu\in\mathcal{P}_{train}} E_{L^2}^{true}(\mu)$ *during the iterations of Algorithm 2 (green stars) and the test error* $\max_{\mu\in\mathcal{P}_{test}} E_{L^2}^{true}(\mu)$ *(blue crosses) for the American put with the Heston model.*

6.3.2. Examples on the Black–Scholes model. Now, we restrict ourselves to the Black–Scholes model. We first demonstrate the parameter and time dependence of our model. In Figure 9, the examples of the primal and dual solutions at different parameter values σ and time steps are presented.

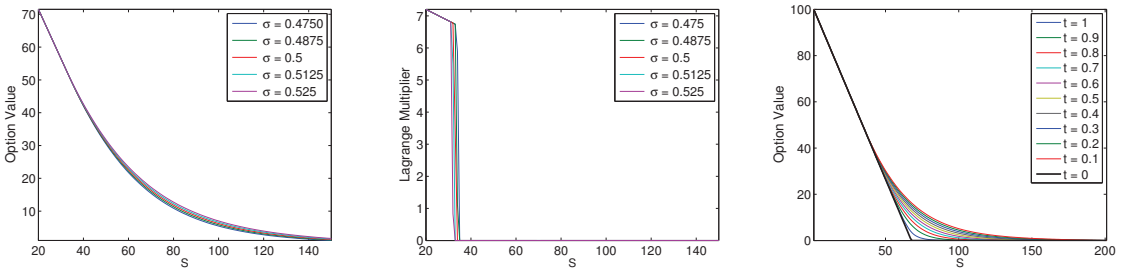

Figure 9. *The primal solutions (left) and corresponding Lagrange multipliers (middle) of the American put option with the Black–Scholes model with different values of the parameter* σ *at a final time step* $t = T$*. The evolution of the solution for different times (right).*

For the next set of experiments, we consider the performance of the RB approach using Algorithm 2 with the true energy error $E(\mu) = E_{energy}^{true}(\mu)$. We construct the bases using the proposed algorithm with $N_V = 50$, $N_W = 25$ and test the RB approach first for a random value of the parameter $\mu = (4.8470 \cdot 10^{-2}, 7.6785 \cdot 10^{-3}, 4.1856 \cdot 10^{-1}) \in \mathcal{P} \setminus \mathcal{P}_{train}$. Some steps of the simulation are represented in Figure 10. The RB and fine detailed simulation curves are hardly distinguishable, which reveals a good RB approximation.

We then test our algorithm on a larger set of parameters. We consider $\mathcal{P}_{test} \subset \mathcal{P}$, a random set of $|\mathcal{P}_{test}| = 20$ parameters, and estimate the mean value of the error $E_{energy}^{true}(\mu)$ over $\mathcal{P}_{test}$. More precisely, we evaluate $\frac{1}{|\mathcal{P}_{test}|} \sum_{\mu\in\mathcal{P}_{test}} E_{energy}^{true}(\mu)$. The results are plotted in

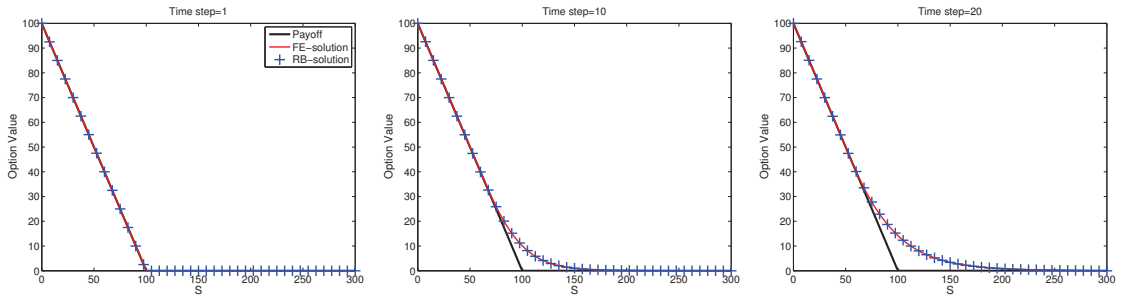

Figure 10. *A finite element (solid red line) and an RB approximation (blue +) at time steps $t/\Delta t = 1$, $t/\Delta t = 10$, and $t/\Delta t = T/\Delta t = 20$ for the American put option with the Black–Scholes model, with $\mu = (4.8470 \cdot 10^{-2}, 7.6785 \cdot 10^{-3}, 4.1856 \cdot 10^{-1})^T$. The payoff function is represented by the black line.*

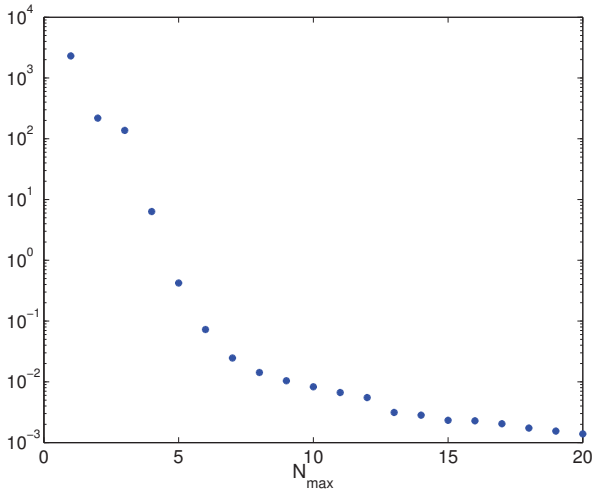

Figure 11. *Values of $\frac{1}{|\mathcal{P}_{test}|} \sum_{\mu \in \mathcal{P}_{test}} E^{true}_{energy}(\mu)$ when using various hierarchical bases obtained with Algorithm 2 for the American put option with the Black–Scholes model.*

the diagram presented in Figure 11. We observe an error decay of several orders in magnitude when simultaneously increasing N_V and N_W.

6.3.3. Efficiency of a posteriori error estimates. We now focus on the efficiency of the design procedure and an inclusion of an a posteriori error estimate using as an example the American put option with the Black–Scholes and Heston models. For this, we consider the POD-Angle-Greedy algorithm and use alternatively $E(\mu) = E^{true}_{energy}(\mu)$ and $E(\mu) = E^{Apost}_{energy}(\mu)$ as selection criterion with $N_{\max} = 25$, i.e., $N_V = 50$, $N_W = 25$ for both models. The other parameter settings remain the same as introduced in sections 6.3.2 and 6.3.1. An illustration of the RB vectors of Ψ_N, Ξ_N for the Black–Scholes model with $E(\mu) = E^{Apost}_{energy}(\mu)$ is shown in Figure 12.

We now comment on an employment of the a posteriori error bounds developed in section 4. We consider the values of the quantity $\max_{\mu \in \mathcal{P}_{train}} E(\mu)$ along the iterations of Algorithm 2, choosing either $E(\mu) = E^{true}_{energy}(\mu)$ or $E(\mu) = E^{Apost}_{energy}(\mu)$. The corresponding results for the

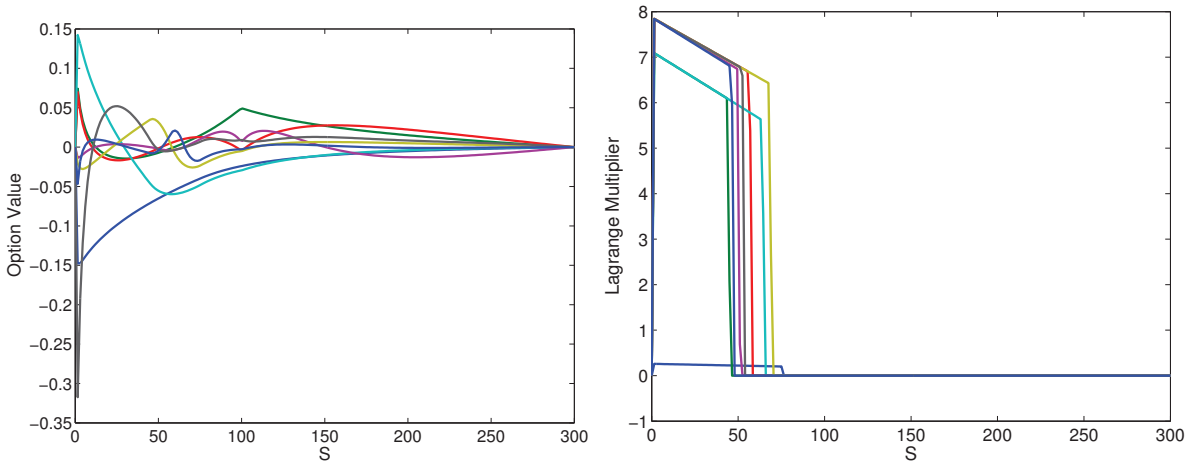

Figure 12. *The first eight vectors of the primal (left) and dual (right) bases obtained with Algorithm 2 with* $E(\mu) = E^{Apost}_{energy}(\mu)$ *for the American put option with the Black–Scholes model.*

Black–Scholes model are presented in Figure 13, and for the Heston model in Figure 14. We observe that for both models, using $E(\mu) = E^{true}_{energy}(\mu)$ as an error measure in Algorithm 2 results in less monotone error convergence of $E^{Apost}_{energy}(\mu)$ with respect to $N_{\max}$, and vice versa. As the variational problem is highly nonlinear, we do not expect exponential convergence as for coercive elliptic problems; hence the error curves are actually expected to flatten with growing N. We interpret the speed of this flattening as indication of the problem difficulty, i.e., nonsmooth solution manifold in contrast to nice smooth elliptic problems. Overall we obtain similar accuracy when using the (cheap) $E^{Apost}_{energy}(\mu)$ measure in contrast to the expensive true error $E^{true}_{energy}(\mu)$, which illustrates the relevance of our a posteriori analysis.

As a measure of the quality of the proposed error estimate, we define the associated effectivities

$$\eta_N(\mu) = \sqrt{\frac{E^{Apost}_{energy}(\mu)}{E^{true}_{energy}(\mu)}}. \tag{6.4}$$

Tables 1 and 2 provide the maximum effectivities $\max_{\mu\in\mathcal{P}_{train}} \eta_N(\mu)$ associated with the error bounds for the Black–Scholes and Heston models using different error measures in the POD-Angle-Greedy algorithm. Note that the choice of $E(\mu)$ in the algorithm does not have a significant impact on the values of the maximum effectivities. We also observe that for the Heston model the effectivity values are higher than for the Black–Scholes one, which can be explained by the more complex nature of the model. Overall the effectivities of two orders of magnitude are acceptable for instationary RB problems.

In order to illustrate the computational efficiency of our approach, we study the runtime performance of the RB method for the case of the Black–Scholes model. The asymptotic speedup obtained when dealing with a large number J of simulations can be estimated by the following formula:

$$\frac{J \cdot t_{full}}{N_{\max} \cdot (t_{full} + |\mathcal{P}_{train}| \cdot (t_{red} + t_{Apost})) + J \cdot t_{red}} \approx \frac{t_{full}}{t_{red}} \approx 180.$$

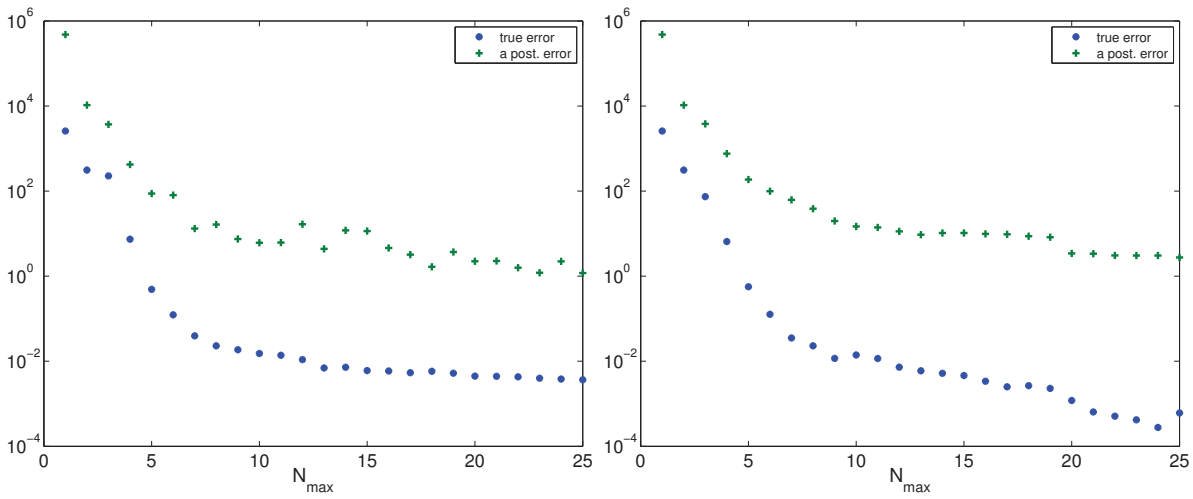

Figure 13. *Evolution of the train error* $\max_{\mu\in\mathcal{P}_{train}} E(\mu)$ *for the American put option with the Black–Scholes model during the iterations of Algorithm 2 with error estimator* $E(\mu) = E^{true}_{energy}(\mu)$ *(left) and with* $E(\mu) = E^{Apost}_{energy}(\mu)$ *(right). Blue stars: values of* $E^{true}_{energy}(\mu)$*; green crosses: values of* $E^{Apost}_{energy}(\mu)$*.*

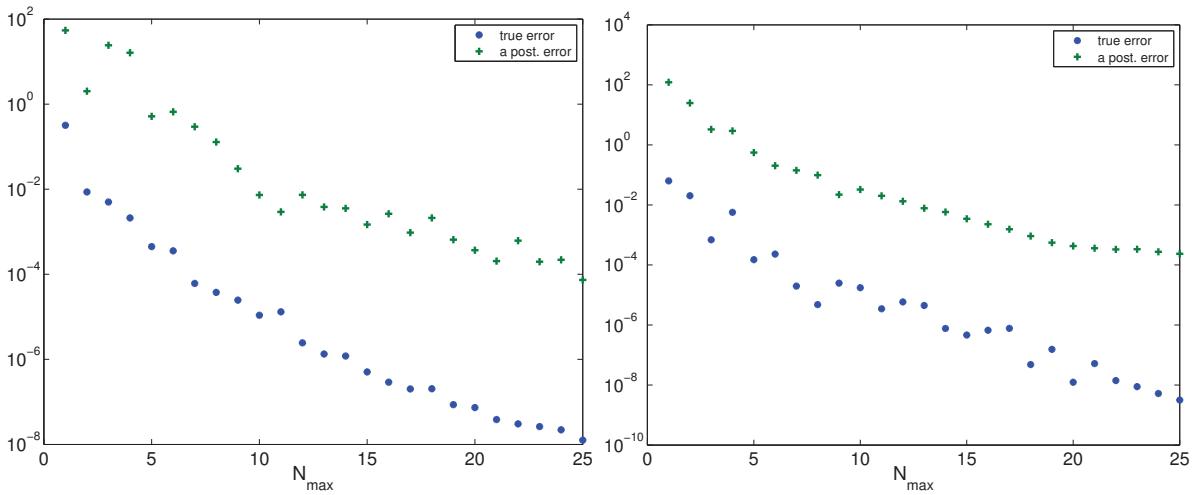

Figure 14. *Evolution of the train error* $\max_{\mu\in\mathcal{P}_{train}} E(\mu)$ *for the American put option with the Heston model during the iterations of Algorithm 2 with error estimator* $E(\mu) = E^{true}_{energy}(\mu)$ *(left) and with* $E(\mu) = E^{Apost}_{energy}(\mu)$ *(right). Blue stars: values of* $E^{true}_{energy}(\mu)$*; green crosses: values of* $E^{Apost}_{energy}(\mu)$*.*

We observe a significant speedup of order 180, when using the RB method. However, this number may vary depending on the performance of the detailed solver and on the dimension of V and W.

From the results of this section, we can conclude that the RB method can be effectively applied for fast evaluation of European and American options. In future, we aim to extend this methodology to real market problems in quantitative finance, in particular to a calibration of model parameters.

Table 1

Maximum effectivities for the American put with the Black–Scholes model at different time steps $n = 5, 10, 15, 20$ *and for different error measures* $E(\mu)$ *and* $N_{\max} = 25$ *in Algorithm 2.*

The choice of $E(\mu) = E^{Apost}_{energy}(\mu)$

$N_{\max}$	(N_V, N_W)	$n = 5$	$n = 10$	$n = 15$	$n = 20$
4	(8, 4)	4.9e+00	5.0e+00	6.2e+00	1.1e+01
8	(16, 8)	4.5e+01	4.3e+01	4.3e+01	4.2e+01
16	(32, 16)	6.4e+01	6.2e+01	6.4e+01	6.5e+01
20	(40, 20)	1.2e+01	7.1e+01	7.9e+01	8.5e+01
24	(48, 24)	6.4e+01	6.7e+01	7.4e+01	1.0e+02

The choice of $E(\mu) = E^{true}_{energy}(\mu)$

$N_{\max}$	(N_V, N_W)	$n = 5$	$n = 10$	$n = 15$	$n = 20$
4	(8, 4)	5.4e+00	6.1e+00	7.2e+00	1.0e+01
8	(16, 8)	5.1e+01	5.3e+01	5.0e+01	4.8e+01
16	(32, 16)	7.3e+01	7.0e+01	7.0e+01	6.3e+01
20	(40, 20)	3.7e+01	5.4e+01	5.1e+01	7.0e+01
24	(48, 24)	3.8e+01	5.1e+01	4.4e+01	7.2e+01

Table 2

Maximum effectivities for the American put with the Heston model at different time steps $n = 5, 10, 15, 20$ *and for different error measures* $E(\mu)$ *and* $N_{\max} = 25$ *in Algorithm 2.*

The choice of $E(\mu) = E^{Apost}_{energy}(\mu)$

$N_{\max}$	(N_V, N_W)	$n = 5$	$n = 10$	$n = 15$	$n = 20$
4	(8, 4)	4.0e+01	6.0e+01	7.1e+01	7.6e+01
8	(16, 8)	6.6e+01	1.1e+02	1.5e+02	1.5e+02
16	(32, 16)	1.2e+02	1.5e+02	1.7e+02	1.7e+02
20	(40, 20)	1.1e+02	1.1e+02	1.5e+02	1.9e+02
24	(48, 24)	1.9e+02	2.4e+02	3.8e+02	3.6e+02

The choice of $E(\mu) = E^{true}_{energy}(\mu)$

$N_{\max}$	(N_V, N_W)	$n = 5$	$n = 10$	$n = 15$	$n = 20$
4	(8, 4)	4.2e+01	6.1e+01	7.6e+01	8.8e+01
8	(16, 8)	4.9e+01	8.7e+01	1.1e+02	1.2e+02
16	(32, 16)	8.6e+01	1.1e+02	1.1e+02	1.2e+02
20	(40, 20)	1.4e+02	1.5e+02	1.5e+02	1.7e+02
24	(48, 24)	1.4e+02	1.9e+02	2.0e+02	2.0e+02

REFERENCES

[1] Y. Achdou and O. Pironneau, *Computational Methods for Option Pricing*, Frontiers Appl. Math. 30, SIAM, Philadelphia, 2005.

[2] M. Balajewicz, D. Amsallem, and C. Farhat, *Projection-Based Model Reduction for Contact Problems*, preprint, Stanford University, 2015.

[3] F. Black and M. S. Scholes, *The pricing of options and corporate liabilities*, J. Political Economy, 81 (1973), pp. 637–654.
[4] P. Bochev, M. Gunzburger, and J. Shadid, *Stability of the SUPG finite element method for transient advection–diffusion problems*, Comput. Methods Appl. Mech. Engrg., 193 (2004), pp. 2301–2323.
[5] D. Boffi, M. Fortin, and F. Brezzi, *Mixed Finite Element Methods and Applications*, Springer Ser. Comput. Math., Springer, Berlin, Heidelberg, 2013.
[6] A. Buffa, Y. Maday, A. T. Patera, C. Prud'homme, and G. Turinici, *A priori convergence of the greedy algorithm for the parametrized reduced basis method*, ESAIM Math. Model. Numer. Anal., 46 (2012), pp. 595–603.
[7] S. Choi, *Algorithms for orthogonal nonnegative matrix factorization*, Neural Networks, 2008, pp. 1828–1832.
[8] R. Cont, N. Lantos, and O. Pironneau, *A reduced basis for option pricing*, SIAM J. Financial Math., 2 (2011), pp. 287–316.
[9] D. J. Duffy, *Finite Difference Methods in Financial Engineering: A Partial Differential Equation Approach*, John Wiley & Sons, 2006.
[10] L. Feng, V. Linetsky, J. Luis Morales, and J. Nocedal, *On the solution of complementarity problems arising in American options pricing*, Optim. Methods Softw., 26 (2011), pp. 813–825.
[11] V. Galiotos, *Stochastic Volatility and the Volatility Smile*, Tech. Report 15, Department of Mathematics, Uppsala University, 2008.
[12] C. Geiger and C. Kanzow, *Theorie und Numerik restringierter Optimierungsaufgaben*, Springer-Lehrbuch Masterclass, Springer, 2002.
[13] A.-L. Gerner, A. Reusken, and K. Veroy, *Reduced Basis A Posteriori Error Bounds for the Instationary Stokes Equations*, preprint, arXiv:1208.5010, 2012.
[14] S. Glas and K. Urban, *Numerical investigations of an error bound for reduced basis approximations of noncoercive variational inequalities*, IFAC-PapersOnLine, 48 (2015), pp. 721–726.
[15] S. Glas and K. Urban, *On noncoercive variational inequalities*, SIAM J. Numer. Anal., 52 (2014), pp. 2250–2271.
[16] R. Glowinski, *Numerical Methods for Nonlinear Variational Problems*, Scientific Computation, Springer, 2008.
[17] M. A. Grepl and A.T. Patera, *A posteriori error bounds for reduced-basis approximations of parametrized parabolic partial differential equations*, M2AN, Math. Model. Numer. Anal., 39 (2005), pp. 157–181.
[18] M. A. Grepl, *Reduced-Basis Approximation and A Posteriori Error Estimation for Parabolic Partial Differential Equations*, Ph.D. thesis, Massachusetts Institute of Technology, 2005.
[19] B. Haasdonk, *Convergence rates of the POD-greedy method*, M2AN Math. Model. Numer. Anal., 47 (2013), pp. 859–873.
[20] B. Haasdonk and M. Ohlberger, *Reduced basis method for finite volume approximations of parametrized linear evolution equations*, M2AN Math. Model. Numer. Anal, 42 (2008), pp. 277–302.
[21] B. Haasdonk, J. Salomon, and B. Wohlmuth, *A Reduced Basis Method for Parametrized Variational Inequalities*, SimTech preprint 2011–17, University of Stuttgart, 2011.
[22] B. Haasdonk, J. Salomon, and B. Wohlmuth, *A reduced basis method for parametrized variational inequalities*, SIAM J. Numer. Anal., 50 (2012), pp. 2656–2676.
[23] B. Haasdonk, J. Salomon, and B Wohlmuth, *A reduced basis method for the simulation of American options*, in Proceedings of ENUMATH 2011, the 9th European Conference on Numerical Mathematics and Advanced Applications (Leicester 2011), Springer, New York, 2013, pp. 821–829.
[24] C. Hager, S. Hüeber, and B. Wohlmuth, *Numerical techniques for the valuation of basket options and its Greeks*, J. Comput. Finance, 13 (2010), pp. 1–31.
[25] S. L. Heston, *A closed-form solution for options with stochastic volatility with applications to bond and currency options*, Rev. Financial Stud., 6 (1993), pp. 327–343.
[26] N. Hilber, O. Reichmann, C. Schwab, and C. Winter, *Computational Methods for Quantitative Finance. Finite Element Methods for Derivative Pricing*, Springer Finance, 2013.
[27] M. Hintermüller, K. Ito, and K. Kunisch, *The primal-dual active set strategy as a semismooth Newton method*, SIAM J. Optim., 13 (2003), pp. 865–888.
[28] J. C. Hull, *Options, Futures, and Other Derivative Securities*, Prentice-Hall, Englewood Cliffs, NJ, 1993.

[29] S. Ikonen and J. Toivanen, *Efficient numerical methods for pricing American options under stochastic volatility*, Numer. Methods Partial Differential Equations, 24 (2008), pp. 104–126.
[30] S. Ikonen and J. Toivanen, *Operator splitting methods for pricing American options under stochastic volatility*, Numer. Math., 113 (2009), pp. 299–324.
[31] K. J. In't Hout and S. Foulon, *ADI finite difference schemes for option pricing in the Heston model with correlation*, Int. J. Numer. Anal. Model., 7 (2010), pp. 303–320.
[32] A. Janek, T. Kluge, R. Weron, and U. Wystup, *FX smile in the Heston model*, in Statistical Tools for Finance and Insurance, Springer, Heidelberg, 2011, pp. 133–162.
[33] N. Kikuchi and J. T. Oden, *Contact Problems in Elasticity: A Study of Variational Inequalities and Finite Element Methods*, Stud. Appl. Math. 8, SIAM, Philadelphia, 1988.
[34] D. Kinderlehrer and G. Stampacchia, *An Introduction to Variational Inequalities and Their Applications*, Classics Appl. Math. 31, SIAM, Philadelphia, 2000. Reprint of the 1980 original.
[35] A. Kunoth, C. Schneider, and K. Wiechers, *Multiscale methods for the valuation of American options with stochastic volatility*, Internat. J. Comput. Math., 89 (2012), pp. 1145–1163.
[36] D. D. Lee and H. S. Seung, *Learning the parts of objects by non-negative matrix factorization*, Nature, 401 (1999), pp. 788–791.
[37] A. Mayerhofer and K. Urban, *A Reduced Basis Method for Parabolic Partial Differential Equations with Parameter Functions and Application to Option Pricing*, preprint, University of Ulm, 2014.
[38] O. Pironneau, *Calibration of options on a reduced basis*, J. Comput. Appl. Math., 232 (2009), pp. 139–147.
[39] O. Pironneau, *Reduced basis for vanilla and basket options*, Risk Decision Anal., 2 (2011), pp. 185–194.
[40] O. Pironneau, *Proper orthogonal decomposition for pricing options*, J. Comput. Finance, 16 (2012), pp. 33–46.
[41] A. Quarteroni and A. Valli, *Numerical Approximation of Partial Differential Equations*, Springer Ser. Comput. Math., Springer, Berlin, Heidelberg, 1994.
[42] D. Rovas, *Reduced-Basis Output Bound Methods for Parametrized Partial Differential Equations*, Ph.D. thesis, Massachusetts Institute of Technology, Cambridge, MA, 2003.
[43] G. Rozza, *Shape Design by Optimal Flow Control and Reduced Basis Techniques: Applications to Bypass Configurations in Haemodynamics*, Ph.D. thesis, EPFL, Lausanne, 2005.
[44] E. Sachs and M. Schu, *Reduced order models (POD) for calibration problems in finance*, in Numerical Mathematics and Advanced Applications, Springer, 2008, pp. 735–742.
[45] R. U. Seydel, *Tools for Computational Finance*, 4th ed., Universitext, Springer-Verlag, Berlin, 2009.
[46] P. Smaragdis, *Non-negative Matrix Factor Deconvolution; Extraction of Multiple Sound Sources from Monophonic Inputs*, in Independent Component Analysis and Blind Signal Separation, C. G. Puntonet and A. Prieto, eds., Lecture Notes in Comput. Sci. 3195, Springer, Berlin, Heidelberg, 2004, pp. 494–499.
[47] K. Veroy, C. Prud'homme, D. V. Rovas, and A. T. Patera, *A posteriori error bounds for reduced-basis approximation of parametrized noncoercive and nonlinear elliptic partial differential equations*, in Proceedings of 16th AIAA Computational Fluid Dynamics Conference, 2003, paper 2003-3847.
[48] A. Weiss and B. Wohlmuth, *A posteriori error estimator and error control for contact problems*, Math. Comp., 78 (2009), pp. 1237–1267.
[49] G. Winkler, T. Apel, and U. Wystup, *Valuation of options in Heston's stochastic volatility model using finite element methods*, Foreign Exchange Risk, (2001), pp. 283–303.
[50] B. Wohlmuth, *A mortar finite element method using dual spaces for the Lagrange multiplier*, SIAM J. Numer. Anal., 38 (2000), pp. 989–1012.
[51] B. Wohlmuth, *Variationally consistent discretization schemes and numerical algorithms for contact problems*, Acta Numer., 20 (2011), pp. 569–734.
[52] Z. Zhang, E. Bader, and K. Veroy, *A Duality Approach to Error Estimation for Variational Inequalities*, preprint, RWTH Aachen, 2014.
[53] R. Zvan, P. A. Forsyth, and K. R. Vetzal, *Penalty methods for American options with stochastic volatility*, J. Comput. Appl. Math., 91 (1998), pp. 199–218.